

Bifurcation of Plasma Balls and Black Holes to Lobed Configurations

Vitor Cardoso,^{1,2} Óscar J. C. Dias,^{3,4}

¹ *CENTRA, Dept. de Física, Instituto Superior Técnico,
Av. Rovisco Pais 1, 1049-001 Lisboa, Portugal*

² *Dept. of Physics and Astronomy, The University of Mississippi,
University, MS 38677-1848, USA*

³ *DAMTP, Centre for Mathematical Sciences, University of Cambridge,
Wilberforce Road, Cambridge CB3 0WA, United Kingdom*

⁴ *Dept. de Física e Centro de Física do Porto, Faculdade de Ciências da Universidade do Porto,
Rua do Campo Alegre 687, 4169 - 007 Porto, Portugal*

vcardoso@fisica.ist.utl.pt, O.Dias@damtp.cam.ac.uk

ABSTRACT

At high energy densities any quantum field theory is expected to have an effective hydrodynamic description. When combined with the gravity/gauge duality an unified picture emerges, where gravity itself can have a formal holographic hydrodynamic description. This provides a powerful tool to study black holes in a hydrodynamic setup. We study the stability of plasma balls, holographic duals of Scherck-Schwarz (SS) AdS black holes. We find that rotating plasma balls are unstable against m -lobed perturbations for rotation rates higher than a critical value. This unstable mode signals a bifurcation to a new branch of non-axisymmetric stationary solutions which resemble a “peanut-like” rotating plasma. The gravitational dual of the rotating plasma ball must then be unstable and possibly decay to a non-axisymmetric long-lived SS AdS black hole. This instability provides therefore a mechanism that bounds the rotation of SS black holes. Our results are strictly valid for the SS AdS gravity theory dual to a SS gauge theory. The latter is particularly important because it shares common features with QCD, namely it is non-conformal, non-supersymmetric and has a confinement/deconfinement phase transition. We focus our analysis in 3-dimensional plasmas dual to SS AdS₅ black holes, but many of our results should extend to higher dimensions and to other gauge theory/gravity dualities with confined/deconfined phases and admitting a fluid description.

Contents

1	Introduction	3
1.1	Dual hydrodynamic description of gravity	3
1.2	A brief summary of our results	5
2	Relativistic hydrodynamic equations	7
2.1	Relativistic hydrodynamic equations	7
2.2	Hydrodynamical and thermal equilibrium conditions. Equation of state	9
2.3	Conserved charges	10
3	Equilibrium solutions: rigidly rotating plasma balls and rings	11
3.1	Plasma Balls	11
3.2	Plasma Rings	12
3.3	The hydrodynamic regime	13
4	Stability analysis of plasma balls and rings.	14
4.1	Perturbations of the equilibrium solutions: inviscid relativistic case	14
4.2	Plasma balls: instability and critical rotation in the inviscid case	16
4.3	Viscosity: instability and critical rotation in the non-relativistic case	18
5	Bifurcation to two-lobed configurations: rotating plasma peanuts	20
6	Unstable plasma balls and their dual black holes	25
7	Acknowledgments	27
A	On the stability of plasma rings	28

1 Introduction

The equations of fluid dynamics and properties of fluids at large have been used for centuries, not only to describe fluids but also as *analogue* models for other more complex phenomena. For instance, early experiments with liquid drops by Plateau [1] were aimed at understanding the effect of gravity on planets (surface tension was then a model for the gravitational force). Another well-known example, is Bohr and Wheeler's [2] proposal to describe nuclear fission as the rupture of a charged liquid drop, where now the surface tension plays the role of nuclear forces. In general relativity, the membrane paradigm, whereby a black hole horizon is mimicked by a stretched fluid membrane, provides another example of the power of analogue models, with useful applications in astrophysical systems. Still in a gravity setup, it was recently suggested to use fluid analogs to explain phenomena observed in general relativistic scenarios, in particular the classical instability of black strings and branes [3]. Accordingly, the gravitational Gregory-Laflamme instability would have a counterpart in the Rayleigh-Plateau instability of fluid mechanics [4, 5] (responsible for the breakup of liquid jets and tubes).

1.1 Dual hydrodynamic description of gravity

The anti-de Sitter/Conformal Field Theory (AdS/CFT) correspondence adds an interesting twist to this story, making these analogies powerful and formal. Indeed, it has emerged with the work of Fermi [6], Landau [7] and others, that often the complicated time dependent dynamics of quantum fields is approximated by a fluid model description. It seems in fact that any gauge theory has a hydrodynamic limit [8, 9]. Combining these ideas together one expects gravity to have a *dual* hydrodynamic description [9]. This expectation has been formally verified in [10, 11], and later in [12, 13], where it was explicitly shown that a gravitational geometry satisfies perturbatively Einstein-AdS gravity to any order as long as the associated holographic stress tensor $T^{\mu\nu}$ (read from the AdS/CFT dictionary) has vanishing spacetime divergence, $\nabla_\nu T^{\mu\nu} = 0$. One recognizes the latter equations as those that govern fluid dynamics. At leading order the stress tensor is that of a perfect fluid; in the next-to-leading order in the perturbation, $T^{\mu\nu}$ gets a contribution that describes viscosity and dissipation effects; at higher order $T^{\mu\nu}$ provides information about the fluid relaxation timescales. Thus Einstein-AdS gravity is indeed dual to hydrodynamics, in the appropriate regime.

The hydrodynamic description of gravity [10, 11, 12, 13] has support on the AdS/CFT duality, relating type IIB string theory on $\text{AdS}_5 \times S^5$ with $\mathcal{N} = 4$ Super Yang-Mills (SYM) gauge theory. SYM differs considerably from QCD. For example, as opposed to SYM, QCD is non-conformal, non-supersymmetric (non-SUSY) and has both a confined and a deconfined phase. Thus, the holy grail of the field is to find a string/QCD duality, which would allow one to study hard non-perturbative phenomena in QCD through a weak-coupling perturbative analysis of the dual string system, and vice-versa. So far this programme has not been completed (see [14, 15] for discussions), however some gravity/gauge dualities are known where the gauge theory shares some important common features with QCD. The simplest example is the Scherk-Schwarz (SS) compactification of a 5-dimensional ($5d$) CFT which yields a $4d$ non-conformal, non-SUSY gauge theory with a

confinement/deconfinement phase transition [16]¹. The original CFT is $5d$ maximally SUSY SYM theory that describes field excitations living in a stack of $D4$ -branes. Identifying periodically one of the worldvolume directions of the $D4$ -branes, imposing anti-periodic boundary conditions for the fermions along this direction, and finally dimensionally reducing along this compact direction one gets the desired SS gauge theory. The gravitational dual description of this system is obtained by taking the appropriate decoupling limit of the geometry describing the near-extremal $D4$ -branes with the compact SS worldvolume direction. Because of the presence of this SS direction there are two solutions: one is a black brane (deconfined gluon phase) and the other one is the AdS-soliton (confined hadronic phase) [19]. The solution that dominates the partition function is the one that minimizes the free energy of the system. One finds that there is a critical temperature T_c - the confinement temperature - above (below) which the black brane (AdS-soliton) minimizes the free energy [16]. The confinement temperature is the one where the Euclidean time circle has the same length as the SS circle. At this confinement temperature the two phases can cohabit in equilibrium separated by a domain wall. Not less important, at this temperature one can have a confinement/deconfinement phase transition in the gauge theory which corresponds in the dual gravity side to a phase transition between the thermal AdS-soliton and the black brane phases [16] (in the context of global AdS backgrounds the transition between thermal global AdS and the Schwarzschild black hole solution is known as Hawking-Page phase transition). Some of these properties are schematically represented in Fig. 1.a). The black hole, solution of the SS compactification of AdS_5 gravity on a circle, that interpolates between the black brane phase and the AdS-soliton confined phase with a domain wall in between is still not known. But in Ref. [20] a numerical solution was found which describes an infinite planar domain wall separating the black brane in one side from the confined AdS-soliton on the other, at the confinement temperature. This solution is expected to describe approximately the near-horizon geometry of the above mentioned black hole solution in the limit where the black hole is large.

Strong arguments suggest that at high energy densities the SS compactification of $5d$ CFT also has a long wavelength effective hydrodynamical description [20]. Indeed, as described two paragraphs above this is certainly true for a CFT, and a similar proof (although necessarily more complicated) should follow similarly for a SS compactification of a CFT. Then, the corresponding gravity/gauge duality, asserts that $3d$ fluid dynamics provides an effective theory describing the SS compactification of AdS_5 gravity in the long wavelength regime [20, 21]. That is, on the boundary of a SS compactification of AdS_5 (asymptoting to $\mathcal{M}^3 \times \mathcal{S}^1$, with \mathcal{S}^1 the distinguished SS circle), the black hole is described by a plasma lump immersed on the vacuum confined phase with a domain wall with surface tension separating the two phases. This is schematically represented in Fig. 1.b). In this description, the black hole horizon maps to the full plasma lump bulk, not to its boundary. The SS circle plays a minor role on the fluid description (meaning that the plasma lumps are translationally invariant along this direction) but as we enter through the radial holographic direction into the bulk, the SS circle must shrink to zero size at the horizon where the domain

¹SS theory has a transition from a hadronic phase to a gluon phase. To have instead a quark-gluon phase at high temperature we need to add fundamental matter to the model. This can be done through the introduction of probe D6-branes [17] or D8-branes [18]. The latter system is known as holographic QCD or Sakai-Sugimoto model. Currently, these gauge systems are the closest to QCD we can have with a theory that has a gravity dual [15].

wall is. This implies that the topology of the corresponding event horizon is given by the fibration of the SS circle S^1 over the plasma lump geometry, with the circle shrinking to a point on the boundary. So, *e.g.*, a plasma ball with a disk topology D^2 corresponds in the bulk to a black hole with horizon topology S^3 , and a plasma ring with topology $S^1 \times I$ is dual to a black ring with topology $S^1 \times S^2$ [21]. To leading order, *i.e.*, without dissipation, the plasma lump is described by a perfect fluid stress tensor with an equation of state characterizing the fluid from which the gauge theory is “made of”. The domain wall contributes with a boundary term, proportional to its surface tension, to the stress tensor. Finally, the system is calibrated in such a way that the confined phase exterior to the plasma lump is vacuum with zero pressure. These plasma balls and plasma rings were studied in great detail in [21] with an emphasis on the AdS_5 case, and the full phase diagram for balls and rings in AdS_6 was obtained more recently in [22].

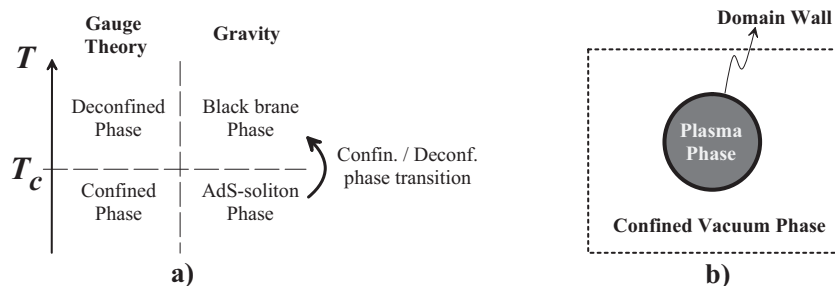


Figure 1: (a) Dominating phases in the gauge theory and in gravity. For temperatures below the confinement temperature T_c , the confined hadronic phase (AdS-soliton in gravity) dominates the partition function, while above T_c the deconfined gluon phase (black brane in gravity) dominates. At T_c the system suffers a first order confinement/deconfinement phase transition. (b) At T_c and in its vicinity, in the dual fluid description on the boundary of the AdS gravity solution, the black hole is described by a plasma phase immersed in the confined vacuum phase and separated by a domain wall with surface tension.

1.2 A brief summary of our results

In the present study we analyze the stability of these plasma lumps, with an emphasis on plasma balls. We find that rotating plasma balls are unstable against m -lobed perturbations (with m being the azimuthal number of the perturbation) if their rotation is higher than a critical value. We further find that the marginal unstable mode is a bifurcation point to a new branch of stationary solutions in the phase diagram of solutions. This new phase describes m -lobed plasma lumps. In the simplest $m = 2$ case we have a 2-lobed configuration which presumably (if we draw from experience with classical incompressible fluids [23, 24, 25]) goes over to a peanut-like configuration for large enough angular momentum. In this work, we shall refer to such solutions interchangeably as rotating *plasma peanut*, or 2-lobed configurations. A phase diagram including also this new family is sketched in Fig. 2. The associated gauge/gravity duality will then be used to predict that black holes asymptoting to a SS compactification of AdS_5 should also be unstable to m -lobed

perturbations. The result of the current study provides a good example of how the hydrodynamic description of gravity can provide a powerful predictive tool to discuss black hole physics and the associated dual gauge theory. Note that although we restrict our analysis to $d = 3$ plasmas dual

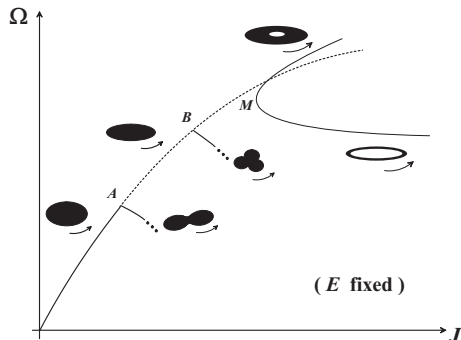


Figure 2: Schematic phase diagram with angular velocity *vs* angular momentum of stationary solutions at fixed energy. The rotating plasma balls and plasma rings (“fat” and “thin” rings merge at point M) phases were already studied in Ref. [21]. Here we find that above a critical rotation (represented by points A , B , ...), plasma balls become unstable against m -lobed perturbations (the unstable balls are represented by a dash line). The marginal point where the instability sets in is a bifurcation point to a new branch of non-axisymmetric m -lobed plasma lumps. In the simplest $m = 2$ case, this is a rotating plasma peanut. This phase diagram summarizes some of our main results, accurately represented in Fig. 7.

to black objects in SS AdS₅, our main results and conclusions should extend to any d -dimensional plasma lump dual to SS AdS _{$d+2$} black objects, and to other gauge/gravity dualities with confined and deconfined phases and admitting a fluid description (see however discussion in Section 6).

The instability of rotating plasma balls could have been guessed from classical works and experiments with rotating fluids [1, 24, 23, 26, 27]. A similar reasoning was recently used [13, 28] to relate the Gregory-Laflamme gravitational instability of black strings and branes to the Rayleigh-Plateau instability of plasma tubes. In the rest of this introduction we describe with some detail the aforementioned classical studies on rotating fluids.

The stability of *incompressible 4d non-relativistic* fluids was studied in detail by Chandrasekhar [23] and later completed by Brown and Scriven [24], for fluids held by surface tension and in the absence of gravity. The analysis was extended in Ref. [5] to a general number of spacetime dimensions. In short these works found the following. Start with a static fluid ball and slowly add rotation. The fluid ball starts to flatten at the poles. One finds a critical rotation frequency Ω_c , after which two or more families can co-exist. One of the families is the axisymmetric one. Proceeding along this family while increasing rotation, one finds a second critical frequency Ω_* at which the ball “pinches” at the origin, and becomes a doughnut like configuration. The axisymmetric family was found to be *unstable* to small perturbations after the point Ω_c . The other family that bifurcates off at Ω_c is a “two-lobed” configuration (see Figs. 1 and 2 in [5]). Close enough to the bifurcation point, this family is *stable* to small perturbations. There are other families, three-lobed, four-lobed, etc,

branching off at different points as one increases rotation. These seem to be always unstable. Recent accurate experiments [26] have confirmed the existence, bifurcation points, and stability properties of these families. This kind of evolution diagram was found to hold also in gravitationally bound (Newtonian) objects with the same qualitative behavior: the Mac-Laurin configuration being the axisymmetric family and the Jacobi sequence, a tri-axial ellipsoid, branching off at the bifurcation point [29].

The plan of the rest of the paper is the following. Section 2 reviews the relativistic hydrodynamic equations, the equilibrium conditions, equation of state, and the conserved charges, that govern a Scherk-Schwarz plasma in a $3d$ Minkowski background (we try to be self-contained). Section 3 then discusses the properties of the axisymmetric lumps of the theory, namely the plasma balls and plasma rings, and discusses the regime of validity of the hydrodynamic description. In Section 4 we discuss in detail the stability of plasma balls, the stability of plasma rings is deferred to Appendix A. In Section 5 we find that the marginal stable mode found in the previous section is a bifurcation point to a new branch of lobed lumps. Section 6 discusses the consequences of these findings to the phase diagram of black hole solutions in SS AdS gravity.

2 Relativistic hydrodynamic equations

Here we review the relativistic hydrodynamic equations governing a Scherk-Schwarz plasma in a $3d$ Minkowski background. We also derive the dissipation contribution to the hydrodynamic equations which are not easy to find in the literature. We will be interested in plasma configurations in mechanical and thermodynamic equilibrium. We follow closely [21, 28].

2.1 Relativistic hydrodynamic equations

Fluid mechanics is an effective description at long distances, valid when the fluid variables vary on distance scales that are large compared to the mean free path l_{mfp} of the system. As a consequence it is natural to expand the stress tensor in powers of derivatives of the four-velocity u^μ . To zeroth order in the derivative expansion, Lorentz invariance and the correct static limit uniquely determine that the stress tensor is the sum of the perfect fluid plus boundary contributions,

$$T_{\text{perf}}^{\mu\nu} = (\rho + P) u^\mu u^\nu + P g^{\mu\nu}, \quad T_{\text{bdry}}^{\mu\nu} = -\sigma h^{\mu\nu} |\partial f| \delta(f). \quad (2.1)$$

Here, u^μ is the fluid velocity, ρ , P and σ are the density, pressure and surface tension of the fluid. The fluid boundary is defined by $f(x^\mu) = 0$, it has unit spacelike normal $n_\mu = \partial_\mu f / |\partial f|$, and $h^{\mu\nu} = g^{\mu\nu} - n^\mu n^\nu$ is the projector onto the boundary.

The first subleading order of the derivative expansion introduces dissipation effects in the problem. Lorentz invariance and the physical requirement that entropy variation is non-negative de-

mands that the dissipation stress tensor is [30]²

$$T_{\text{diss}}^{\mu\nu} = -\zeta\vartheta P^{\mu\nu} - 2\eta\sigma^{\mu\nu} + q^\mu u^\nu + u^\mu q^\nu, \quad (2.2)$$

where ζ is the bulk viscosity, η is the shear viscosity, κ is the thermal conductivity, and (for $d = 3$)

$$\begin{aligned} a^\mu &= u^\nu \nabla_\nu u^\mu, & \vartheta &= \nabla_\mu u^\mu, \\ \sigma^{\mu\nu} &= \frac{1}{2} \left(P^{\mu\lambda} \nabla_\lambda u^\nu + P^{\nu\lambda} \nabla_\lambda u^\mu \right) - \frac{1}{2} \vartheta P^{\mu\nu}, & q^\mu &= -\kappa P^{\mu\nu} (\partial_\nu \mathcal{T} + a_\nu \mathcal{T}), \end{aligned} \quad (2.3)$$

are the acceleration, expansion, shear viscosity tensor, and heat flux, respectively. The last equation is the relativistic Fourier law.

The hydrodynamic equations describe the conservation of the stress tensor,

$$\nabla_\mu \left(T_{\text{perf}}^{\mu\nu} + T_{\text{bdry}}^{\mu\nu} + T_{\text{diss}}^{\mu\nu} \right) = 0. \quad (2.4)$$

It then follows that in the presence of dissipation, the relativistic continuity, Navier-Stokes and Young-Laplace equations, are respectively given by³

$$u^\mu \nabla_\mu \rho + (\rho + P)\vartheta = \zeta\vartheta^2 - q^\mu a_\mu - \nabla_\mu q^\mu + 2\eta\sigma^{\mu\nu} \nabla_\mu u_\nu, \quad (2.5)$$

$$\begin{aligned} (\rho + P)a^\nu &= -P^{\mu\nu} \nabla_\mu P + \zeta (P^{\mu\nu} \nabla_\mu \vartheta + \vartheta u^\mu \nabla_\mu u^\nu) + 2\eta (\nabla_\mu \sigma^{\mu\nu} - u^\nu \sigma^{\mu\alpha} \nabla_\mu u_\alpha) \\ &\quad - (q^\mu \nabla_\mu u^\nu + \vartheta q^\nu + u^\mu \nabla_\mu q^\nu - q^\mu a_\mu u^\nu), \quad \text{with } P^{\mu\nu} \equiv g^{\mu\nu} + u^\mu u^\nu, \end{aligned} \quad (2.6)$$

$$\left[P - \zeta\vartheta + 2\eta \left(\frac{1}{2}\vartheta + u^\mu n^\alpha \nabla_\alpha n_\mu \right) \right]_{>}^{<} = \sigma K, \quad \text{with } K \equiv h_\mu{}^\nu \nabla_\nu n^\mu, \quad (2.7)$$

where $P^{\mu\nu}$ is the projector onto the hypersurface orthogonal to u^μ , K is the boundary's extrinsic curvature, and $[Q]_{>}^{<} \equiv Q_{<} - Q_{>}$ is the jump on a quantity Q when we cross the boundary from the interior into the exterior of the plasma (we will be interested in the case where the plasma object is immersed in vacuum; then the outside contribution in the lhs of (2.7) vanishes). In the derivation of Eq. (2.7), the constraint that the fluid velocity must be orthogonal to the boundary normal is used (this guarantees that the fluid is confined inside the boundary),

$$u^\mu n_\mu = 0. \quad (2.8)$$

For a conformal plasma it is well-known that the bulk viscosity coefficient vanishes, $\zeta = 0$, and that the ratio of the shear viscosity η to the entropy density s of the plasma is $\frac{\eta}{s} = \frac{1}{4\pi}$. However, our system is described by a Scherk-Schwarz plasma that is not conformal and the dissipation coefficients satisfy the relations $\zeta > 0$, $\frac{\eta}{s} > \frac{1}{4\pi}$ and $\kappa > 0$.

²At leading order the entropy current density is $(J_S^\mu)_{\text{perf}} = s u^\mu$ and is conserved. In the first subleading order, one gets the extra dissipative contribution $(J_S^\mu)_{\text{diss}} = \frac{q^\mu}{\mathcal{T}}$. The entropy current density $J_S^\mu = (J_S^\mu)_{\text{perf}} + (J_S^\mu)_{\text{diss}}$ is no longer conserved and satisfies $\mathcal{T} \nabla_\mu J_S^\mu = \frac{q^\mu q_\mu}{\kappa \mathcal{T}} + \zeta \vartheta^2 + 2\eta \sigma_{\mu\nu} \sigma^{\mu\nu} > 0$ as long as η, ζ and κ are positive parameters, as we assume [21]. In equilibrium, $\nabla_\mu J_S^\mu$ must vanish. It follows that, q^μ , θ and $\sigma^{\mu\nu}$ must vanish in equilibrium.

³To go from (2.4) into (2.5)-(2.7) note that (2.4) reduces to a volume and a boundary contributions. The latter gives the Young-Laplace equation while the former yields the Continuity and Navier-Stokes equations. To get these we use $\nabla_\mu \Theta(-f) = -(\partial_\mu f)$, $\nabla_\mu \delta(f) = -|\partial f| n_\mu \delta(f)$, $u_\nu u^\nu = -1$, $h^{\mu\nu} n_\mu = 0$, $P^{\mu\nu} u_\mu = 0$, $u_\nu a^\nu = 0$, $u^\mu n_\mu = 0$, $q^\mu u_\mu = 0$, $\sigma^{\mu\nu} u_\mu = 0$, $u^\mu u_\mu = -1$, $n^\mu n_\mu = 1$, and $\nabla_\alpha g^{\mu\nu} = 0$. We also use properties of the type: $n_\nu n^\nu = 1$ implies $n_\nu n^\mu \nabla_\mu n^\nu = 0$.

2.2 Hydrodynamical and thermal equilibrium conditions. Equation of state

In this subsection we briefly review some general results derived in Ref. [28] valid for equilibrium and general (non-)axisymmetric plasma configurations. We focus our discussion on fluids in a $3d$ Minkowski background⁴ with stationarity timelike Killing vector $\xi = \partial_t$ and spacelike Killing vector $\chi = \partial_\phi$, but the results of [28] were derived for a general background geometry.

A fluid with local entropy density s and local temperature \mathcal{T} satisfies the Euler relation and the Gibbs-Duhem relation given, respectively, by

$$\rho + P = \mathcal{T}s, \quad dP = sd\mathcal{T}, \quad (2.9)$$

where the latter relation follows from differentiating the former relation and use of the first law of thermodynamics. Using these relations and demanding hydrodynamic (*i.e.*, mechanical) equilibrium we find that the plasma must also be in thermodynamic equilibrium [28]. So, equilibrium plasma configurations must satisfy the hydrodynamic equations discussed in the previous subsection with vanishing subleading dissipation and diffusion contributions. It then follows that any stationary fluid configuration with local temperature \mathcal{T} must have a velocity given by

$$u = \frac{\mathcal{T}}{T} (\xi - \Omega\chi). \quad (2.10)$$

with constant T and Ω . So stationary configurations are rigidly rotating equilibrium solutions with constant plasma temperature T related to the local temperature \mathcal{T} by the Lorentz factor (we use $u^2 = -1$),

$$\gamma = \frac{\mathcal{T}}{T} = [-(\xi - \Omega\chi)^2]^{-1/2}, \quad (2.11)$$

which is the redshift factor relating measurements done in the laboratory and comoving frames.

Combining the Euler relation (2.9) and the Young-Laplace equation (equation (2.7) without the dissipative terms), we can relate the plasma temperature T to a combination of several magnitudes at the fluid surface,

$$T = \frac{\sigma K + \rho}{\gamma s}. \quad (2.12)$$

We see that T is *not* simply proportional to the surface tension or to the mean curvature, although it grows linearly with both [28]. For a static fluid K will be constant over the surface, but in a stationary configuration K is not a constant along the boundary. In the duality to a black hole, T corresponds to the Hawking temperature of the horizon.

A universal behavior of fluids is that they always pick boundary configurations which reduce their potential energy for a fixed volume. For static solutions, this implies that the area of the fluid surface is minimized. For stationary solutions, the potential energy not only has a surface tension term but also a centrifugal contribution. In Ref. [28] it was shown that this variational principle still holds for relativistic fluids and that the minimization problem is equivalent to maximize the plasma entropy while keeping its energy and angular momenta fixed. In the gravitational dual system black holes satisfy the variational principle that their entropy is extremized for fixed energy

⁴We use polar coordinates (t, r, ϕ) , and the non-vanishing affine connections are $\Gamma_{\phi\phi}^r = -r$ and $\Gamma_{r\phi}^\phi = \Gamma_{\phi r}^\phi = 1/r$.

and angular momenta. In the duality between SS-AdS black holes and fluid lumps, the entropy, energy and angular momentum are identified on both sides, while the temperature is mapped according to (2.12). Note that unexpectedly (because it looks *a priori* to be a contradiction), the analysis of Ref. [28] shows that maximization of the black hole horizon area is equivalent, for static configurations, to minimization of the fluid surface area. The reason for this equivalence can be traced back to the fact that the black hole horizon is mapped to the entire volume of the plasma and not to the plasma boundary.

The results quoted so far are independent of the equation of state for the fluid. The gravitational/hydrodynamic duality where we frame our analysis requires however a particular equation of state. Indeed, we are interested in the long wavelength limit of a Scherk-Schwarz compactification of a 4d CFT. The 3d (non-conformal) plasma that results from the dimensional reduction of the 4d conformal plasma has equation of state defined by [21]

$$P = \frac{\rho - 4\rho_0}{3}, \quad \rho + P = \frac{4}{3}(\rho - \rho_0), \quad s = 4\alpha^{1/4} \left(\frac{\rho - \rho_0}{3} \right)^{\frac{3}{4}}, \quad \mathcal{T} = \left(\frac{\rho - \rho_0}{3\alpha} \right)^{\frac{1}{4}}. \quad (2.13)$$

with ρ_0 and α constants. This equation of state is valid in or out of equilibrium and is normalized such that the vacuum pressure vanishes. For the SS plasma in equilibrium, it follows from (2.11) and (2.13) that the pressure and energy density satisfy the relations

$$P = \frac{\rho_*}{3} \gamma^4 - \rho_0, \quad \rho = \rho_* \gamma^4 + \rho_0, \quad (2.14)$$

where ρ_* is a constant.

2.3 Conserved charges

The constituent fluid of the plasma object has local energy density ρ , pressure P , velocity u^μ , local entropy density s , and local temperature \mathcal{T} . These *local* quantities provide the information we need to compute the thermodynamic quantities (energy, angular momentum, entropy, temperature) of the plasma balls and plasma rings.

To define these quantities recall that our fluid lives in a 3d Minkowski background with stationarity timelike Killing vector $\xi = \partial_t$ and spacelike Killing vector $\chi = \partial_\phi$. We can then foliate the spacetime into constant t hypersurfaces Σ_t and ξ^μ is their unit normal vector. Then, given any Killing vector ψ^μ , one can define the associated conserved charges $\mathcal{Q}[\psi] = \int_{\Sigma_t} dV T_{\mu\nu} \xi^\mu \psi^\nu$, where dV is the induced volume measure on Σ_t . The fluid velocity is given by (2.10), *i.e.*, $u^\mu = \gamma (\delta^{\mu t} + \Omega \delta^{\mu\phi})$ with $\gamma = (1 - r^2 \Omega^2)^{-1/2}$. The energy and angular momentum of the plasma associated, respectively, with the Killing vectors ξ and χ are then

$$\begin{aligned} E &= \int_V dV [\gamma^2 (\rho + r^2 \Omega^2 P) + \sigma |\partial f| \delta(f)], \\ J &= \int_V dV r^2 \Omega \gamma^2 (\rho + P) - \sigma \int_{\Sigma_t} dV h_{\mu\nu} \xi^\mu \chi^\nu |\partial f| \delta(f). \end{aligned} \quad (2.15)$$

Note that for axisymmetric solutions (plasma balls and plasma rings) the boundary term in J proportional to σ vanishes. It is however present for non-axisymmetric solutions where $\chi \cdot n \neq 0$

(i.e., when the fluid boundary is not invariant under the action of χ) [28]. The total entropy of the fluid is the conserved charge associated to the entropy density current su^μ ,

$$S = - \int_V dV (\chi \cdot u)s = \int_V dV \gamma s. \quad (2.16)$$

3 Equilibrium solutions: rigidly rotating plasma balls and rings

There are three families of axisymmetric rigidly rotating equilibrium configurations in a $3d$ Minkowski background: plasma balls, plasma rings and plasma tubes. The later were already analyzed in a previous paper and do not interest us here [28]. The plasma balls and rings were discussed in detail in [21]. Because we will later study the stability of these solutions we review here their properties, following closely [21].

Consider plasma configurations in a $d = 3$ Minkowski background parametrized by coordinates (t, r, ϕ) . The axisymmetry requirement demands that the boundaries of the plasma depend only on r . Each boundary is thus defined by the condition (j specifies a particular boundary in the case where more than one is present)

$$f(r) = r - R_j = 0, \quad (3.1)$$

and has unit normal $n_\mu = \frac{\partial_\mu f}{|\partial f|} = \delta_{\mu r}$. Its extrinsic curvature $K = h_\mu^\nu \nabla_\nu n^\mu$ is $K = \frac{1}{R_j}$.

Following [21], it is convenient to frame our discussion in terms of the dimensionless variables,

$$\tilde{\Omega} = \frac{\sigma \Omega}{\rho_0}, \quad \tilde{r} = \frac{\rho_0 r}{\sigma}, \quad v = \Omega r = \tilde{\Omega} \tilde{r}, \quad (3.2)$$

and also to use dimensionless thermodynamic quantities,

$$\tilde{E} = \frac{\rho_0 E}{\pi \sigma^2}, \quad \tilde{J} = \frac{\rho_0^2 J}{\pi \sigma^3}, \quad \tilde{S} = \frac{\rho_0^{5/4} S}{\pi \alpha^{1/4} \sigma^2}, \quad \tilde{T} = T \left(\frac{\alpha}{\rho_0} \right)^{1/4}. \quad (3.3)$$

We now consider the properties of plasma balls and rings.

3.1 Plasma Balls

Plasma balls are characterized by having a single axisymmetric outer surface at $r = R_o$ and by $P_{>} = 0$. Using equation of state (2.13), the Young-Laplace boundary condition (2.7) reads

$$\rho(R_o) = 4\rho_0 + \frac{3\sigma}{R_o}. \quad (3.4)$$

Plasma balls in equilibrium must satisfy the equation of state (2.14) and obey the boundary condition (3.4). This implies that

$$\frac{\rho(v) - \rho_0}{3\rho_0} (1 - v^2)^2 = \left(1 + \frac{\tilde{\Omega}}{v_o} \right) (1 - v_o^2)^2 \equiv g_+(v_o). \quad (3.5)$$

The range of v is $[0, 1]$ and $\rho(v) - \rho_0$ is always positive for the plasma ball. This is in agreement with the requirement that the local temperature defined in (2.13) must be positive. After using the equation of state (2.13) and (3.5) we get for the local plasma temperature,

$$\mathcal{T} = \gamma \left(\frac{\rho_0 g_+(v_o)}{\alpha} \right)^{1/4}. \quad (3.6)$$

For later use note that the constant ρ_* introduced in (2.14) is related to ρ_0 by

$$\rho_* = 3\rho_0 g_+(v_o). \quad (3.7)$$

This relation follows from replacing (2.14) in the Young-Laplace equation.

Use of (3.5) and (2.13) in (2.15)-(3.3) yields for the dimensionless energy, angular momentum and entropy of the plasma ball,

$$\tilde{E} = \frac{4v_o^2 - v_o^4 + 5\tilde{\Omega}v_o - \tilde{\Omega}v_o^3}{\tilde{\Omega}^2}, \quad \tilde{J} = \frac{2v_o^4 + 2\tilde{\Omega}v_o^3}{\tilde{\Omega}^3}, \quad \tilde{S} = \frac{4v_o^2}{\tilde{\Omega}^2} \sqrt{1 - v_o^2} \left(1 + \frac{\tilde{\Omega}}{v_o} \right)^{3/4}, \quad (3.8)$$

while the dimensionless temperature and dimensionless angular velocity of the plasma balls are

$$\tilde{T} = \left(\frac{\partial \tilde{E}}{\partial \tilde{S}} \right)_{\tilde{J}} = [g_+(v_o)]^{1/4}, \quad \tilde{\Omega} = \left(\frac{\partial \tilde{E}}{\partial \tilde{J}} \right)_{\tilde{S}}. \quad (3.9)$$

Note that the plasma ball temperature is the redshifted local temperature, $T = \mathcal{T}/\gamma$, in agreement with the discussion associated with (2.11). The plasma angular velocity is naturally the same as the fluid one with no associated Lorentz factor.

3.2 Plasma Rings

These have an axisymmetric inner surface at $r = R_i$ (where $P_< = 0$), in addition to the outer surface at $r = R_o$ (where $P_> = 0$). Using equation of state (2.13), the Young-Laplace equation yields the pair of boundary conditions,

$$\rho(R_o) = 4\rho_0 + \frac{3\sigma}{R_o}, \quad \rho(R_i) = 4\rho_0 - \frac{3\sigma}{R_i}. \quad (3.10)$$

Plasma rings in equilibrium must also satisfy the equation of state (2.14) and obey the boundary conditions (3.10). This means that rings must satisfy the pair of equations

$$\begin{aligned} \frac{\rho(v) - \rho_0}{3\rho_0} (1 - v^2)^2 &= \left(1 + \frac{\tilde{\Omega}}{v_o} \right) (1 - v_o^2)^2 \equiv g_+(v_o) \\ &= \left(1 - \frac{\tilde{\Omega}}{v_i} \right) (1 - v_i^2)^2 \equiv g_-(v_i). \end{aligned} \quad (3.11)$$

Note that $\rho(v) - \rho_0$, and thus the local temperature are non-negative as long as $v_i \geq \tilde{\Omega}$. This system can be satisfied only when

$$g_+(v_o) = g_-(v_i). \quad (3.12)$$

This condition constrains the three variables v_o , v_i and $\tilde{\Omega}$ as, *e.g.*, $v_i = v_i(v_o, \tilde{\Omega})$. An inspection of $g_+(v_o) = g_-(v_i)$ concludes that there is a minimum v_o , call it v_o^* , above which (3.12) is valid [21]. So, plasma rings exist only for $v_o \geq v_o^*$. In fact there are two families of black rings. One is called the fat plasma ring and exists for $\tilde{\Omega} \leq v_i \leq v_i^*$ (where $v_i^* < v_o^*$ is such that the derivative of $g_-(v_i)$ vanishes), while the second, dubbed as thin plasma ring, exists for $v_i^* \leq v_i \leq 1$. At $v_i = v_i^*$ the two families meet at a regular solution.

Use of (2.13) and (3.12) yields for the local plasma temperature

$$\mathcal{T} = \gamma \left(\frac{\rho_0 g_+(v_o)}{\alpha} \right)^{1/4} = \gamma \left(\frac{\rho_0 g_-(v_i)}{\alpha} \right)^{1/4}. \quad (3.13)$$

Finally note that ρ_* defined in (2.14) is related to ρ_0 by $\rho_* = 3\rho_0 g_+(v_o) = 3\rho_0 g_-(v_i)$.

Using (3.11) and (2.13) in (2.15)-(3.3) yields for the dimensionless energy, angular momentum and entropy

$$\begin{aligned} \tilde{E} &= \frac{4(v_o^2 - v_i^2) - (v_o^4 - v_i^4) + 5\tilde{\Omega}(v_o + v_i) - \tilde{\Omega}(v_o^3 + v_i^3)}{\tilde{\Omega}^2}, & \tilde{J} &= \frac{2(v_o^4 - v_i^4) + 2\tilde{\Omega}(v_o^3 + v_i^3)}{\tilde{\Omega}^3}, \\ \tilde{S} &= \frac{4}{\tilde{\Omega}^2} \left[v_o^2 \sqrt{1 - v_o^2} \left(1 + \frac{\tilde{\Omega}}{v_o} \right)^{3/4} - v_i^2 \sqrt{1 - v_i^2} \left(1 - \frac{\tilde{\Omega}}{v_i} \right)^{3/4} \right], \end{aligned} \quad (3.14)$$

while the dimensionless temperature and dimensionless angular velocity of the plasma rings are

$$\tilde{T} = \left(\frac{\partial \tilde{E}}{\partial \tilde{S}} \right)_{\tilde{J}} = [g_+(v_o)]^{1/4} = [g_-(v_i)]^{1/4}, \quad \tilde{\Omega} = \left(\frac{\partial \tilde{E}}{\partial \tilde{J}} \right)_{\tilde{S}}. \quad (3.15)$$

Note that to determine the plasma ring family of solutions, the constraint (3.12) must be imposed. The different equilibrium configurations are best understood by looking at a phase diagram of solutions shown in later sections.

3.3 The hydrodynamic regime

Relativistic hydrodynamics provides a good effective description of the deconfined plasma phase of $\mathcal{N} = 4$ Yang Mills theory compactified down to $d = 3$ on a Scherk-Schwarz circle only if certain conditions are satisfied [21]. First, hydrodynamics is by definition valid when the thermodynamic quantities of the fluid vary slowly over the mean free path ℓ_{mfp} of the fluid. In our case $\ell_{\text{mfp}} \sim T_c \sim \frac{\rho_0}{\sigma}$. A good estimate for the validity regime is obtained when the maximum fractional rate of change of the fluid local temperature, $\frac{\delta T}{T}|_{\text{max}} \sim \partial_r \ln \gamma|_{\text{max}}$ (recall that $\mathcal{T} = T\gamma$) is much smaller than ℓ_{mfp} . This occurs for $\frac{\tilde{\Omega} v_o}{1 - v_o^2} \ll 1$. This condition is satisfied by a wide range of plasma balls and rings as long as we are away from extremality. Second, the analysis done so far and onwards assumes that surface tension is constant, $\sigma = \sigma(T_c)$, when in fact it is a function of the fluid temperature at the surface. This assumption is valid when $\mathcal{T}/T_c \sim 1$ at the boundary surfaces. This is the case for a long range of energies and angular momentum as long as we do not approach too much the extremal configurations. Finally, the boundary of the plasma is treated as a delta-like surface when in fact it has a thickness of order T_c^{-1} . So the analysis is valid when the boundary radius is everywhere large when compared with T_c^{-1} , $\{R_o, R_i, R_o - R_i\} \gg \frac{\sigma}{\rho_0}$. This is the case if the plasma energy is large and again if we are away from the extremal configurations [21].

4 Stability analysis of plasma balls and rings.

In this section we want to consider a rigidly rotating plasma ball in $d = 3$ and address its stability when perturbed. The dynamics of the perturbations is dictated by the hydrodynamic equations, subject to appropriate boundary conditions. In this section we restore light velocity factors to ease comparison between relativistic and classical results.

4.1 Perturbations of the equilibrium solutions: inviscid relativistic case

Perturbations take the plasma away from thermal equilibrium and therefore viscosity and diffusion effects start to contribute. The energy-momentum tensor of the fluid includes not only the perfect fluid and the boundary surface tension terms (2.1), but also a dissipative contribution (2.2). For now, we neglect the dissipation contribution to the fluid stress tensor.

Consider then a generic equilibrium solution described by velocity $u_{(0)}^\mu = \gamma (\delta^{\mu t} + \Omega \delta^{\mu \phi})$ (with $\gamma = (1 - r^2 \Omega^2 / c^2)^{-1/2}$), pressure and density functions as given by (2.14), which we label with the subscript (0), standing for unperturbed quantities. Now, suppose the system acted upon by a perturbation with the generic form

$$\begin{aligned}
 P &= P_{(0)} + \delta P, & \delta P(t, r, \phi) &= \epsilon \gamma^4 \mathcal{P}(r) e^{(\omega - im\Omega)t + im\phi}, \\
 \rho &= \rho_{(0)} + \delta \rho, & \rho_{(0)} &= \frac{3}{c^2} P_{(0)} + 4\rho_0, & \delta \rho(t, r, \phi) &= \frac{3}{c^2} \delta P(t, r, \phi), \\
 u^\mu &= u_{(0)}^\mu + \delta u^\mu, & \delta u^\mu(t, r, \phi) &= \epsilon \left(U_t(r) \delta^{\mu t} + \gamma^{-3} U_r(r) \delta^{\mu r} + \frac{U_\phi(r)}{r} \delta^{\mu \phi} \right) e^{(\omega - im\Omega)t + im\phi},
 \end{aligned} \tag{4.1}$$

where we used the equation of state (2.13) valid also out of equilibrium and we denote the perturbation of a quantity Q as δQ . Positive real part of ω signals an instability. After eliminating the 0th order terms using the unperturbed hydrodynamic equations, the continuity and the Navier-Stokes equations yield, up to first order in the perturbation,

$$\begin{aligned}
 c^2 u_{(0)}^\mu \nabla_\mu \delta \rho + c^2 \delta u^\mu \nabla_\mu \rho_{(0)} + (\rho_{(0)} c^2 + P_{(0)}) \nabla_\mu \delta u^\mu + (c^2 \delta \rho + \delta P) \nabla_\mu u_{(0)}^\mu &= 0, \\
 (\rho_{(0)} c^2 + P_{(0)}) \left(\delta u^\mu \nabla_\mu u_{(0)}^\nu + u_{(0)}^\mu \nabla_\mu \delta u^\nu \right) + (c^2 \delta \rho + \delta P) u_{(0)}^\mu \nabla_\mu u_{(0)}^\nu \\
 + \left(g^{\mu\nu} + u_{(0)}^\mu u_{(0)}^\nu \right) \nabla_\mu \delta P + \left(\delta u^\nu u_{(0)}^\mu + u_{(0)}^\nu \delta u^\mu \right) \nabla_\mu P_{(0)} &= 0.
 \end{aligned} \tag{4.2}$$

which reads

$$0 = \frac{3\gamma r \omega}{\frac{4\rho_*}{3} c^2} \mathcal{P} + \gamma^{-3} \frac{d}{dr} (r U_r) + r(\omega - im\Omega) U_t + im U_\phi, \tag{4.3}$$

$$0 = \frac{i\gamma \Omega}{\frac{4\rho_*}{3} c^2} (i\omega \Omega r^2 - mc^2 \gamma^{-2}) \mathcal{P} - 2\Omega^2 r \gamma^{-1} U_r - c^2 \omega U_t, \tag{4.4}$$

$$0 = \frac{\gamma^2}{\frac{4\rho_*}{3}} \mathcal{P}' + \omega U_r - 2\gamma^3 \Omega U_\phi, \tag{4.5}$$

$$0 = \frac{i\gamma}{\frac{4\rho_*}{3} c^2} (i\omega \Omega r^2 - mc^2 \gamma^{-2}) \mathcal{P} - 2\Omega r \gamma^{-1} U_r - \omega r U_\phi, \tag{4.6}$$

where $\mathcal{P}' \equiv \frac{d\mathcal{P}}{dr}$. Multiplying (4.6) by Ω and subtracting (4.4) it follows that $U_t = \frac{r\Omega}{c^2}U_\phi$, which satisfies the requirement that $u_\mu u^\mu = -c^2$ up to order ϵ . These equations can be used to get a second order ODE for \mathcal{P} , and another equation defining U_r in terms of \mathcal{P} and its derivative. The later is

$$U_r(r) = \frac{-2i\Omega [c^2 m - r^2 \Omega (i\omega + m\Omega)] \gamma^2 \mathcal{P}(r) - c^2 \omega r \mathcal{P}'(r)}{\frac{4\rho_*}{3} r [-\omega^2 r^2 \Omega^2 + c^2 (\omega^2 + 4\Omega^2)]}, \quad (4.7)$$

while the second order ODE for \mathcal{P} is

$$\begin{aligned} 0 = & -r^2 c^6 \gamma^{-4} (c^2 \omega^2 \gamma^{-2} + 4c^2 \Omega^2) \mathcal{P}'' - r c^6 \gamma^{-4} (\omega^2 (c^2 + \Omega^2 r^2) + 4c^2 \Omega^2) \mathcal{P}' \\ & + \left[c^8 m^2 (\omega^2 + 4\Omega^2) - \omega^2 r^8 \Omega^6 (\omega - im\Omega)^2 + c^4 r^4 \Omega^2 (6i\omega^3 m \Omega - 7\omega^4 + 2\omega^2 \Omega^2 (3m^2 - 14) + 24i\omega m \Omega^4) \right. \\ & - c^2 r^6 \Omega^4 (6i\omega^3 m \Omega - 5\omega^4 + 4\omega^2 (m^2 - 2)\Omega^2 + 12i\omega m \Omega^3 + 4m^2 \Omega^4) \\ & \left. + c^6 r^2 (3\omega^4 - 2i\omega^3 m \Omega - 4\omega^2 (m^2 - 5)\Omega^2 - 12i\omega m \Omega^3 + 4(8 - 3m^2)\Omega^4) \right] \mathcal{P} \end{aligned} \quad (4.8)$$

The perturbed continuity and Navier-Stokes equations must be supplemented by appropriate boundary conditions. For that, let us write a general boundary disturbance as

$$r = R(t, \phi), \quad \text{with} \quad R(t, \phi) = R_j \left(1 + \epsilon \chi e^{(\omega - im\Omega)t + im\phi} \right), \quad \epsilon \ll 1, \quad (4.9)$$

where R_j is the unperturbed radius of the boundary. For the plasma ball one has $R_j \equiv R_o$, while for the plasma ring we have both the inner and outer boundaries: $R_j \equiv R_i$ and $R_j \equiv R_o$. For plasma rings, this reduces the possible set of perturbations to the subsector with similar temporal and angular deformations in both boundaries.

The first boundary condition is a kinematic condition requiring that the normal component of the fluid velocity on the boundary satisfies the perturbed version of (2.8), $u_{(0)}^\mu \delta n_\mu + \delta u^\mu n_\mu^{(0)} = 0$, where $\delta n_\mu \equiv n_\mu|_{R(t,\phi)} - n_\mu^{(0)}$ and the unperturbed normal is $n_\mu^{(0)} \equiv n_\mu|_{R_{o,i}} = \delta_\mu^r$. This ensures that the fluid is confined inside the boundary and is also a consistency relation between the boundary and the velocity perturbation. To leading order this boundary condition reads,

$$\text{BC I:} \quad U_r|_{R_{o,i}} \simeq \omega \gamma_{o,i}^4 R_{o,i} \chi_{o,i}. \quad (4.10)$$

The second boundary condition is a balance on the normal stress at the boundary. This means that the pressure perturbation must also satisfy the perturbed version of the Young-Laplace equation (2.7), namely: $\delta P_{<} - \delta P_{>} = \sigma \delta K$. Since we have vacuum in the exterior of the plasma configuration this reads

$$\text{BC II:} \quad \left(P_{\leq}^{(0)}|_{R(t,\phi)} + \delta P|_{R_{o,i}} \right) - P_{\leq}^{(0)}|_{R_{o,i}} = \pm \sigma \left(K|_{R(t,\phi)} - K|_{R_{o,i}} \right),$$

where the choices $\{<, +, o\}$ apply to the outer boundary and $\{>, -, i\}$ to the inner boundary, if present. The subscript $r = R(t, \phi)$ means that we evaluate the expression at the perturbed boundary $r = R(t, \phi)$ defined in (4.9) and the subscript $r = R_{o,i}$ means evaluation at the unperturbed boundary $r = R_{o,i}$. $P_{\leq}^{(0)}$ is computed using (2.14). The extrinsic curvature $K = h_\mu^\nu \nabla_\nu n^\mu$ is obtained using the unit normal of (4.9),

$$n_\mu = |\delta f|^{-1} \left(-R'_t \delta_\mu^t + \delta_\mu^r - R'_\phi \delta_\mu^\phi \right), \quad |\delta f| = \left(1 - \frac{1}{c^2} R_t'^2 + \frac{1}{r^2} R_\phi'^2 \right)^{\frac{1}{2}}. \quad (4.11)$$

The Young-Laplace equation (4.10) then yields to leading order in ϵ

$$\mathcal{P}|_{R_{o,i}} \simeq \frac{\sigma}{R_{o,i}} \chi_{o,i} \gamma_{o,i}^{-4} \left[\pm \left(\frac{1}{c^2} (\omega - im\Omega)^2 R_{o,i}^2 + m^2 - 1 \right) - \Sigma \gamma_{o,i}^6 \right], \quad (4.12)$$

where \pm applies, respectively, to the outer and inner boundary and $\gamma_{o,i} \equiv \gamma|_{R_{o,i}}$. Here, we have defined the rotational Bond parameter Σ which plays an important role in this problem. It measures the competition between centrifugal and surface tension effects and is defined by,

$$\Sigma \equiv \frac{4\rho_*}{3} R_{o,i}^3 \frac{\Omega^2}{\sigma}. \quad (4.13)$$

4.2 Plasma balls: instability and critical rotation in the inviscid case

We now particularize the above framework for plasma balls. We can combine boundary conditions (4.12) and (4.10) in a single condition,

$$U_r(R_o) = \frac{\omega R_o^2 \gamma_o^8}{\sigma \left(m^2 - 1 - \Sigma \gamma_o^6 + \frac{R_o^2}{c^2} (\omega - im\Omega)^2 \right)} \mathcal{P}(R_o). \quad (4.14)$$

To summarize, (4.7) and (4.14) give us a condition on \mathcal{P} . Together with regularity conditions at the origin, Eq. (4.8) is then an eigenvalue problem for ω .

Although we will present our numerical results in full generality, it is insightful to compare them with the small rotation regime where an analytical treatment is possible. In this small velocity regime, $\Omega R_o \ll c$, (4.8), (4.7) and (4.14) reduce respectively to

$$\frac{1}{r} \frac{d}{dr} (r\mathcal{P}') - \frac{m^2}{r^2} \mathcal{P} = 0, \quad (4.15)$$

$$U_r(r) = -\frac{2im\Omega\mathcal{P}(r) + \omega r\mathcal{P}'(r)}{\frac{4\rho_*}{3} r (\omega^2 + 4\Omega^2)}, \quad (4.16)$$

$$U_r(R_o) = \frac{\omega R_o^2}{\sigma (m^2 - 1 - \Sigma)} \mathcal{P}(R_o). \quad (4.17)$$

If we define

$$\Sigma_\omega \equiv \frac{4\rho_*}{3} R_o^3 \omega^2, \quad (4.18)$$

we can express the analytical solution to the system (4.15)-(4.17) as

$$\sqrt{\Sigma_\omega} = i\sqrt{\Sigma} \pm \sqrt{(m-1)(\Sigma - m(m+1))}. \quad (4.19)$$

Thus, for $\Sigma > m(m+1)$ and $m \geq 2$, the system is unstable. This is one of our main results: in the simplest $m = 2$ case, plasma balls become unstable against 2-lobed or peanut-like deformations when the rotation reaches a critical value Ω_{crit} . For higher rotation they become also unstable against m -lobed deformations, with $m > 2$. Notice that in the non-relativistic regime the density is approximately a constant and equal to $4\rho_*/3$ (see footnote 5). Thus, our result (4.19) is precisely the well-known result for inviscid, incompressible fluids of density $\rho = 4\rho_*/3$ [31].

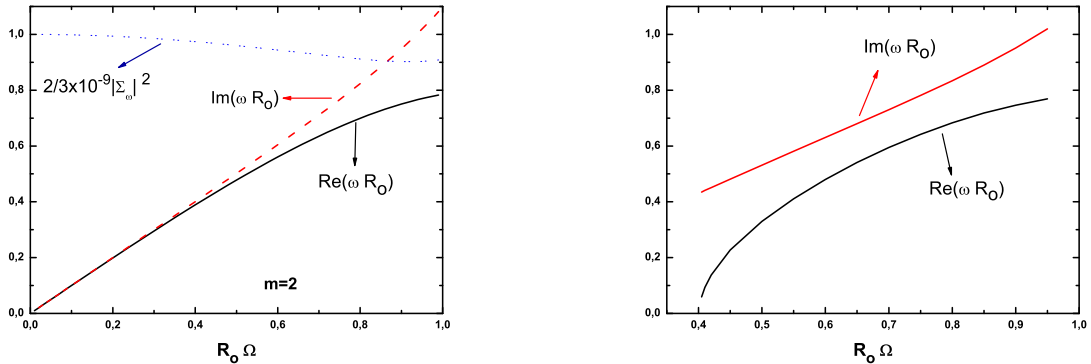


Figure 3: Left Panel: Details of instability for the $m = 2$ mode. We are fixing $\Sigma = \frac{4}{3} \times 10^9$, $\sigma = 10^{-7}$. Classically, *i.e.*, for small rotation rates, the quantity Σ_ω is a constant, and both the real and imaginary part of the characteristic frequency ω lie on the straight line, *i.e.*, directly proportional to Ω . The stability region lies in a range of very small ΩR_o , not visible in the figure. Right Panel: Details of the instability for the $m = 2$ mode, this time with parameters chosen such that the instability sets in at large ΩR_o . In this case, the threshold is around $\Omega R_o/c \sim 0.402$, the parameters are $\frac{4\rho_* R_o}{3\sigma} = 24$. Classically, the threshold would be at $\Omega R_o/c = 0.5$.

Our numerical results for the relativistic system (4.8), (4.7) and (4.14), are depicted in Fig. 3 for the $m = 2$ case. For small rotation rates, they are in perfect agreement with the non-relativistic limit (4.19). We find a (in any case small) deviation from the classical prediction only when $\Omega R_o/c$ approaches unity. In the right panel, we show a case where the threshold rotation frequency at which an instability sets in is rather large. For these values we get a threshold of approximately $\Omega R_o/c \sim 0.402$, still in good agreement with the classical result $\Omega R_o/c = 0.5$, as given by (4.19) for these values ($\frac{4\rho_* R_o}{3\sigma} = 24$). We were not able to find unstable modes for $m = 1$, in agreement with the classical result (4.19) for small rotations.

The critical rotation frequency $R_o \Omega_{\text{crit}}$, for which the configuration is marginally stable is shown in Figure 4. For a given $\rho_* R_o/\sigma$ and rotations larger than $R_o \Omega_{\text{crit}}$, the system is unstable to two lobed perturbations ($m = 2$). We find that for moderately large $\rho_* R_o/\sigma \geq 50$, the classical formula (4.19) holds.

At this point we should check if and when the lengthscale of the instability falls within the hydrodynamic limit (discussed in the end of Section 3). The thermodynamic quantities of the fluid must vary slowly over the mean free path of our system, $\ell_{\text{mfp}} \sim T_c \sim \frac{\rho_0}{\sigma}$. The lengthscale of the instability is the ratio of its wavelength to the tube's radius and is of order $(\omega R_o^2)^{-1}$. Therefore the hydrodynamic description is valid for instabilities that satisfy $\omega R_o \gg \frac{\sigma}{\rho_0 c^2 R_o}$. A simple inspection of Fig. 4 allows one to conclude that the conditions for a hydrodynamic description are satisfied in the non-relativistic limit where $\frac{\rho_* c^2 R_o}{\sigma} \gtrsim 50$. It is certainly satisfied for very large values of $\frac{\rho_0 c^2 R_o}{\sigma}$. In addition, the initially unperturbed plasma ball must of course satisfy the conditions discussed already in the end of Section 3.

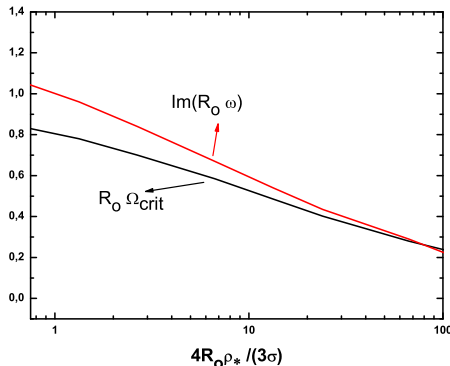


Figure 4: Critical rotation frequency ΩR_o at which instability sets in, as a function of the dimensionless quantity $\frac{4\rho_* R_o}{3\sigma}$. For large $\frac{4\rho_* R_o}{3\sigma}$, the classical prediction (4.19) applies.

4.3 Viscosity: instability and critical rotation in the non-relativistic case

Although we start with a plasma ball in thermodynamic equilibrium, viscosity contributions have to be taken into account in the perturbed configuration. In fact even the most “perfect” known fluids have a certain non-vanishing viscosity [32], and this is certainly the case for the SS plasma. It turns out that, for the problem at hand, even a vanishingly small viscosity has a dramatic effect on the critical rotation at which instability sets in. In fact, viscosity introduces a singular-limit, where the “limit of theory is not the theory of the limit” (see [31, 33] for the classical analysis). Thus our relativistic analysis of the previous subsection must address also viscosity effects.

Fortunately, from the full relativistic analysis of the previous section, we know that we can to a good approximation address the present problem in the small rotation regime. To define precisely this regime, recall that in section 3.3 we concluded that hydrodynamics provides a good effective description of the deconfined plasma phase immersed in the vacuum confined phase when the plasma satisfies the condition

$$\frac{\sigma}{\rho_0 c^2 R_o} \ll 1. \quad (4.20)$$

Moreover, in the previous subsection we found that the full (numerical) results for the marginally stable mode (where the m -lobed instability set in) agree very well with the (analytical) non-relativistic results obtained for

$$\frac{\Omega R_o}{c} \ll 1. \quad (4.21)$$

We are therefore justified to use the small velocity regime: in this case not only the non-relativistic results reveal very good agreement with the full relativist analysis but also this is the relevant regime where the hydrodynamic analysis provides valuable information for the dual gravitational system.

The non-relativistic limit of the hydrodynamic equations presented in subsection 2.1 was studied in great detail in [34]. There it is found that the continuity and Navier-Stokes equations reduce,

respectively, to

$$\begin{aligned}\nabla \cdot \mathbf{v} &= 0, \\ \partial_t \mathbf{v} + (\mathbf{v} \cdot \nabla) \mathbf{v} &= -\frac{3}{4\rho_*} \nabla P + \nu \nabla^2 \mathbf{v}, \quad \nu \equiv \frac{3\eta}{4\rho_*},\end{aligned}\tag{4.22}$$

where one uses $u \rightarrow (1, \mathbf{v})$, and ∇_i ($i = r, \phi$) represents the covariant derivative with respect to the purely spatial metric η_{ij} . So in the non-relativistic limit, the hydrodynamic system reduces to the continuity and Navier-Stokes equations for an incompressible fluid with constant density $\rho|_{\gamma=1}$ (so the continuity equation simply states that the velocity field is a solenoid vector: its spatial divergence vanishes), and with kinematical viscosity ν ⁵.

At this point we can now perturb (4.22) and simply follow the classical analysis of the m -lobed instability of a fluid ball done *e.g.*, in [31]. Using the same non-relativistic version of the perturbations used in (4.2), we get,

$$\begin{aligned}\frac{d}{dr}(r U_r) + im U_\phi &= 0, \\ \omega U_r - 2\Omega U_\phi + \frac{3}{4\rho_*} \mathcal{P}' &= \nu \left(U_r'' + \frac{1}{r} U_r' - \frac{(m^2 + 1)}{r^2} U_r - \frac{2im}{r^2} U_\phi \right), \\ \frac{3}{4\rho_*} \frac{im}{r} \mathcal{P} + 2\Omega U_r + \omega U_\phi &= \nu \left(U_\phi'' + \frac{1}{r} U_\phi' - \frac{(m^2 + 1)}{r^2} U_\phi + \frac{2im}{r^2} U_r \right).\end{aligned}\tag{4.23}$$

These equations must now be supplemented by the appropriate boundary conditions. The constraint (2.8) is still valid as well as the associated boundary condition (4.10). The Young-Laplace equation gets now a contribution from the viscous term, and so the normal stress-balance at the boundary, (4.12), is modified to

$$\mathcal{P}|_{R_o} \simeq \frac{\sigma}{R_o} \chi_o \left[(m^2 - 1) - \frac{4\rho_*}{3} \frac{\Omega^2 R_o^3}{\sigma} \right] + 2\nu U_r' .\tag{4.24}$$

Finally, we must also require that the tangential stresses vanish at the boundary (this amounts to require that the fluid is shearless at the boundary), which yields the extra boundary condition

$$R_o^2 U_\phi' - R_o U_\phi - im U_r = 0.\tag{4.25}$$

We can use the first relation in (4.23) to express U_ϕ in terms of U_r and its derivative and then use the remaining equations to solve for U_r and \mathcal{P} . One gets a fourth-order differential equation. In any case, the procedure is trivial and one ends up with the following eigenvalue equation [31]

$$\beta^4 + 2\beta^2 \left((m^2 - 1) - m(m - 1)^2 \frac{\beta^2}{\Phi} - iRe \right) + m Re^2 \left(\frac{m^2 - 1}{\Sigma} - 1 \right) = 0,\tag{4.26}$$

⁵It follows from (3.5) and (3.7) that in the non-relativistic limit one has $\rho \sim \frac{4}{3}\rho_* \sim 4\rho_0$. Moreover, in this limit one finds that a possible contribution coming from the bulk viscosity in the Navier-Stokes vanishes because it is proportional to $\nabla \cdot \mathbf{v}$, and the absence of the particle number conservation and the use of the Landau frame [10] allow to avoid the use of thermal conductivity [34].

where we defined

$$Re \equiv \frac{R_o^2 \Omega}{\nu}, \quad \beta^2 \equiv \frac{\omega}{\Omega} Re, \quad \Phi \equiv \beta^2 + 2m - 2\beta \frac{I_{m-1}(\beta) + I_{m+1}(\beta)}{2I_m(\beta)}. \quad (4.27)$$

Here $I_m(\beta)$ is a modified Bessel function and Re is the Reynolds number. Solving for this eigenvalue equation, we get the behavior depicted in Fig. 5. What the figure shows, and can be proven be

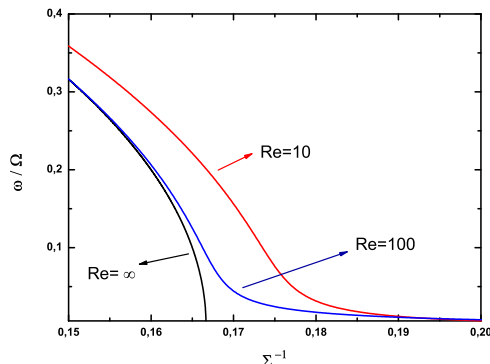


Figure 5: Instability as a function of the inverse of the Bond number, Σ^{-1} for different values of the Reynolds number $Re = 10, 100$ and for $m = 2$. We also show the inviscid values. Notice that the critical Bond number is *not* $m(m+1)$ when viscosity is present, even in the limit where it vanishes. In the general viscous case, the instability is limited by the critical point $\Sigma_c = m^2 - 1$.

proven analytically [31], is that the limit of small viscosity, $Re \rightarrow \infty$, does *not* yield the zero viscosity result. This is quite an astonishing result: the critical Bond number Σ_c when viscosity is introduced is at $\Sigma_c = m^2 - 1$ that is always smaller than the critical value for the instability found in the last subsection, namely, $m(m+1)$. Therefore, the configuration is unstable at *lower* rotation frequencies, when viscosity is accounted for. This result holds for both large and small Reynolds number.

In Fig. 6 we represent the plasma rings, and stable and unstable plasma balls in two distinct phase diagrams at fixed energy⁶, and it summarizes one of our main results.

5 Bifurcation to two-lobed configurations: rotating plasma peanuts

In the previous section we found that plasma balls are marginally stable at $\Sigma_c = m^2 - 1$, when perturbed by an azimuthal mode m . Such a marginal mode usually signals a branching off to another family of solutions, and here it is no exception. This new family is a *non-axisymmetric*

⁶In these diagrams we choose to fix the dimensionless energy at the value $\tilde{E} = 40$ to make a connection with the value chosen in [21], where plasma balls and rings were first discussed. This value of the energy corresponds to $\frac{\rho_* c^2 R_o}{\sigma} \sim 14$. In this case the non-relativistic analysis for the marginal point mismatches the accurate full relativistic result by a factor of approximately 20%.

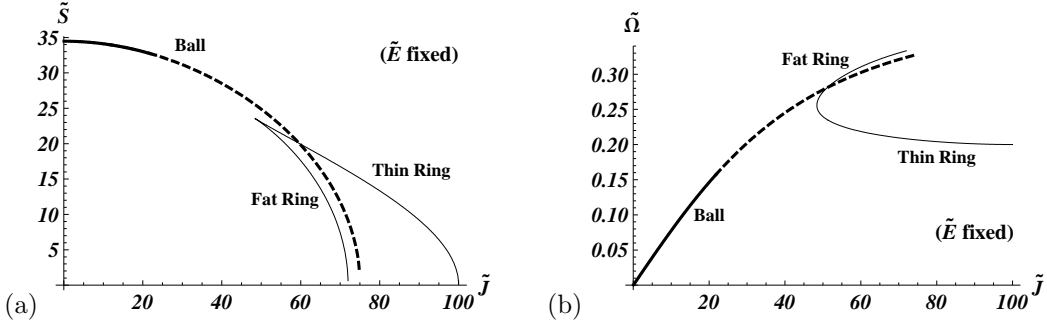


Figure 6: (a) Phase diagram with the entropy of plasma balls and plasma rings \tilde{E} as a function of angular momentum \tilde{J} , at fixed energy $\tilde{E} = 40$ in $d = 3$ [21]. For this value of the energy, one has $v_o^* \simeq 0.7248999$ and $v_i^* \simeq 0.5009615$. Plasma rings exist only for $v_o \geq v_o^*$. The fat plasma rings exist for $\tilde{\Omega}(v_o = 1) \leq v_i \leq v_i^*$ (with $\tilde{\Omega}(v_o = 1) = 0.333333$), while the thin plasma rings exist for $v_i^* \leq v_i \leq 1$. At $v_i = v_i^*$ the two families meet in a regular solution. Hydrodynamics does not provide a good dual description for configurations near extremality ($T = 0$) where the entropy also vanishes. We find that plasma balls become unstable above the critical rotation $\tilde{J}_c \simeq 21.8127$, and the dashed line represents the unstable plasma balls. (b) Similar to Fig a), but this time we represent the phase diagram with the angular velocity $\tilde{\Omega}$ of plasma balls and plasma rings as a function of angular momentum \tilde{J} , at fixed energy, $\tilde{E} = 40$.

m-lobed configuration: a rotating *plasma peanut*. In this section we want to verify the existence of this branch of solutions and study some of its main properties. A detailed numerical study of the full branch of this new plasma phase is outside of the main scope of this work. Here, we will address the most important region, namely we investigate how this family looks close to the bifurcation point $\Sigma = \Sigma_c$ in the phase diagram of stationary solutions. Consistent with the analysis of previous sections we restrict our analysis to the hydrodynamic and small rotation regime, Eqs. (4.20) and (4.21), where the hydrodynamic analysis provides valuable information for the dual gravitational system. We can then follow closely the analysis done by Benner, Basaran and Scriven [33]. In the following we obtain the new branch of rotating plasma peanuts that emerges from the plasma ball bifurcation point.

The energy, angular momentum and entropy of the plasma lump are given by (2.15) and (2.16). In the regime (4.20) and (4.21) (see also footnote 5 and note that $\rho c^2 + P \sim 4\rho_0 c^2$) and in the close vicinity of the plasma ball bifurcation point the associated dimensionless charges read,

$$\begin{aligned}
 \tilde{E} &= \frac{\rho_0 c^2}{\pi \sigma^2} \int_V T^{tt} \approx \frac{4}{\pi} \int_0^\pi d\phi \tilde{R}^2(\epsilon, \phi), \\
 \tilde{S} &= \frac{(\rho_0 c^2)^{5/4}}{\pi \alpha^{1/4} \sigma^2} \int_V \gamma s \approx \frac{4}{\pi} \int_0^\pi d\phi \tilde{R}^2(\epsilon, \phi), \\
 \tilde{J} &= \frac{\rho_0^2 c^5}{\pi \sigma^3} \int_V r^2 T^{t\phi} \approx \frac{2}{\pi} \int_0^\pi d\phi \tilde{\Omega}(\epsilon) \tilde{R}^2(\epsilon, \phi).
 \end{aligned} \tag{5.1}$$

In these relations we are looking for the unknown family of lobed solutions by expanding around the

known plasma ball at the marginal stability point $\Sigma_c = m^2 - 1$. We take ϵ to be the parameter that measures the deviation from the rotating axisymmetric plasma ball with dimensionless radius \tilde{R}_0 , and $\tilde{R}(\epsilon, \phi)$ describes the non-axisymmetric boundary of the unknown plasma peanut (note that in the vicinity of the bifurcation point the axisymmetric deviation is really small and the perturbative approach is appropriate). We also assume that there is mirror symmetry around the $\phi = 0, \pi$ axis.

In a perturbative analysis, known as power series method [33], we now take the boundary radius and Bond parameter to be described by the expansion around the marginally stable plasma ball,

$$\begin{aligned}\tilde{R}(\epsilon, \phi) &= \tilde{R}_0 \left(1 + \epsilon f^{(1)}(\phi) + \frac{\epsilon^2}{2} f^{(2)}(\phi) \right) + \mathcal{O}(\epsilon^3), \\ \Sigma(\epsilon) &= \Sigma_c + \epsilon \Sigma^{(1)} + \frac{\epsilon^2}{2} \Sigma^{(2)} + \mathcal{O}(\epsilon^3).\end{aligned}\tag{5.2}$$

We also introduce the dimensionless pressure jump Π at the axis of rotation (see (2.14)), and its expansion,

$$\Pi \equiv \frac{R_0 c^2}{\sigma} \left(\frac{1}{3} \rho_* - \rho_0 \right), \quad \Pi(\epsilon) = \Pi_c + \epsilon \Pi^{(1)} + \frac{\epsilon^2}{2} \Pi^{(2)} + \mathcal{O}(\epsilon^3).\tag{5.3}$$

The perturbed quantities characterize the m -lobed branch. We want to find a family of configurations that have fixed energy. Perturbations have to solve a total of four equations, namely: the Young-Laplace equation, the energy constraint (we want to represent the branch of solutions in a phase diagram at fixed energy), the orthogonality equations and a equation defining the amplitude parameter ϵ .

The perturbed n^{th} order Young-Laplace equation, $\delta P_{<} = \sigma \delta K$, yields

$$f_{\phi\phi}^{(n)} + (1 + \Sigma_c) f^{(n)} + \Pi^{(n)} = S_{YL}^{(n)},\tag{5.4}$$

where $f_{\phi} \equiv \partial_{\phi} f$ and the relevant source terms S_{YL}^n are

$$\begin{aligned}S_{YL}^{(0)} &= 0, \quad S_{YL}^{(1)} = 0, \quad S_{YL}^{(2)} = (2 - \Sigma_c) \left(f^{(1)} \right)^2 - 2\Sigma^{(1)} f^{(1)} + \left(f_{\phi}^{(1)} \right)^2 + 4f^{(1)} f_{\phi\phi}^{(1)}, \\ S_{YL}^{(3)} &= -3\Sigma^{(2)} f^{(1)} + 3(2 - \Sigma_c) f^{(1)} f^{(2)} + 3 \left(f_{\phi}^{(1)} f_{\phi}^{(2)} - 6(f^{(1)})^2 f_{\phi\phi}^{(1)} \right) \\ &\quad + 6 \left(f^{(1)} f_{\phi\phi}^{(2)} + f^{(2)} f_{\phi\phi}^{(1)} \right) + 9f_{\phi\phi}^{(1)} (f_{\phi}^{(1)})^2 - 6(f_{\phi}^{(1)})^3 - 9f^{(1)} (f_{\phi}^{(1)})^2.\end{aligned}\tag{5.5}$$

The condition that fixes the energy follows from perturbation of the first relation in (5.1), $\delta \tilde{E} = 0$, which yields

$$\int_0^{\pi} d\phi f^{(n)} = S_E^{(n)},\tag{5.6}$$

with source terms

$$S_E^{(0)} = 0, \quad S_E^{(1)} = 0, \quad S_E^{(2)} = - \int_0^{\pi} d\phi \left(f^{(1)} \right)^2, \quad S_E^{(3)} = 3 \int_0^{\pi} d\phi f^{(1)} f^{(2)}.\tag{5.7}$$

For $n \geq 2$ the problem is inhomogeneous and the solution must satisfy an orthogonality condition⁷,

$$\int_0^{\pi} d\phi f^{(1)} S_{YL}^{(n)} + 2\Pi^{(1)} S_E^{(n)} = 0.\tag{5.8}$$

⁷To get (5.8) start with the Young-Laplace equation (5.4). Multiply it by $f^{(1)}(\phi)$; integrate over ϕ ; do a double integration by parts (use the symmetry condition $f^{(n)}(0) = f^{(n)}(\pi)$ and the $n = 1$ Young-Laplace to simplify some of the terms); and finally make use of the energy conservation (5.6).

Finally, the amplitude parameter ϵ is defined as the integral-weighted difference between plasma shapes,

$$\epsilon \equiv \int_0^\pi d\phi f^{(1)}(\tilde{R} - \tilde{R}_o) \rightarrow \int_0^\pi d\phi f^{(1)} f^{(n)} = \delta_n^1. \quad (5.9)$$

The solution of (5.4)-(5.9), up to second order in the perturbation, is

$$\begin{aligned} f^{(1)}(\phi) &= \sqrt{\frac{2}{\pi}} \cos(m\phi), \\ f^{(2)}(\phi) &= \frac{3}{\pi} \left(1 - \frac{1}{m^2}\right) + \frac{2}{\pi} \left(\frac{1}{m^2} - 1\right) \cos^2(m\phi) + \frac{2}{\pi} \left(\frac{2}{m^2} - 3\right) \sin^2(m\phi), \\ \Sigma &= (m^2 - 1) + \frac{\epsilon^2}{2} \frac{3}{2\pi} \frac{(m^4 - 1)(1 - m^2)}{m^2}, \\ \Pi &= 1 - \frac{m^2 - 1}{2} + \frac{\epsilon^2}{2} \frac{3}{\pi} (1 - m^2). \end{aligned} \quad (5.10)$$

These perturbations keep the energy of the stationary solutions fixed and equal to $\tilde{E} = 4\tilde{R}_o^2$. Moreover, use of these relations in the definition (4.13) of the Bond parameter and in (5.1) yields the expansion of the other thermodynamic quantities around the bifurcation point,

$$\begin{aligned} \tilde{\Omega} &= \tilde{R}_o^{-3/2} \sqrt{m^2 - 1} \left(\frac{1}{2} - \epsilon^2 \frac{3(m^4 - 1)}{16m^2\pi} \right) + \mathcal{O}(\epsilon^3), \\ \tilde{J} &= \tilde{R}_o^{5/2} \sqrt{m^2 - 1} \left(1 + \epsilon^2 \frac{3 + 32m^2 - 3m^4}{8\pi m^2} \right) + \mathcal{O}(\epsilon^3), \\ \tilde{S} &= 4\tilde{R}_o^2 + \mathcal{O}(\epsilon^3). \end{aligned} \quad (5.11)$$

This expansion allows to represent the new branch of non-axisymmetric plasma peanuts in a phase diagram of stationary solutions at fixed energy. Since rotation is the mechanism responsible for the instability that signals the bifurcation to the new phase, it is appropriate to represent the 2-lobed plasma lump in a phase diagram that represents the angular momentum \tilde{J} against its conjugated chemical potential $\tilde{\Omega}$. To check the accuracy of our approximations we first observe that at zero order, we have $\tilde{J}^{(0)} = 2\tilde{R}_o^4 \tilde{\Omega} = \frac{2}{16} \tilde{E}^2 \tilde{\Omega}$. For the slope of the plasma ball at the bifurcation point we thus get $\frac{d\tilde{\Omega}^{(0)}}{d\tilde{J}^{(0)}} = \frac{1}{200}$ for $\tilde{E} = 40$. This value is in reasonable agreement with the exact relativistic value for the $\tilde{\Omega} - \tilde{J}$ slope at the bifurcation, obtained from (3.8) (for $\tilde{E} = 40$ we get numerically $\frac{d\tilde{\Omega}^{(0)}}{d\tilde{J}^{(0)}} \sim \frac{1.2}{200}$; as explained in footnote 6 the disagreement is due to the fact that the system with $E = 40$ is not exactly within the classical regime). We can now use the next-to-leading order non-vanishing contribution to get the desired slope for the m -lobed branch, yielding

$$\left(\frac{d\tilde{\Omega}}{d\tilde{J}} \right)^{(2)} = -\frac{24(m^4 - 1)}{3 + 32m^2 - 3m^4} \frac{1}{\tilde{E}^2}. \quad (5.12)$$

For $m = 2$ this is the slope at which the 2-lobed or plasma peanut branch emerges from the plasma ball bifurcation point. In the phase diagram $\tilde{\Omega} - \tilde{J}$ of stationary solutions at fixed energy, represented in Fig. 7, the plasma peanut branch bends down and to the right relatively to the plasma ball family. In this diagram we identify the critical unstable point where bifurcation occurs

and we represent by a dashed line the plasma balls rotating faster than the critical velocity, which are therefore unstable.

This figure summarizes the main result of this section: we have confirmed the existence of a new phase of non-axisymmetric stationary solutions and we were able to use perturbative methods around the bifurcation point to find what is the direction that the new branch of solutions takes relatively to the known phases. A full description of the 2-lobed branch well away from the bifurcation point (where it acquires a well defined peanut shape) would require a full numerical analysis and we leave it for future work. Note also that keeping going up along the plasma ball branch this time already in the unstable ball region to 2-lobed perturbations we would find a succession of new bifurcation points to new phases of solutions representing m -lobed plasma lumps with $m > 2$. The slope of these branches is given by (5.12).

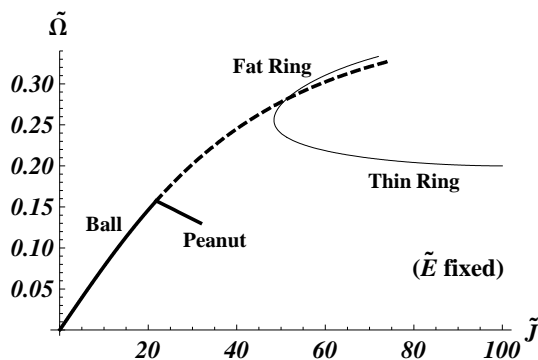


Figure 7: Phase diagram $\tilde{\Omega}(\tilde{J})$ of stationary plasma solutions with fixed energy, $\tilde{E} = 40$. At $(\tilde{J}_c, \tilde{\Omega}_c) \simeq (21.81, 0.157)$ the plasma ball becomes unstable and bifurcates to a branch of rotating plasma peanuts. We show this branch in the vicinity of the bifurcation point but it continues for larger values of \tilde{J} . Note that the bifurcation point for plasma balls is at lower angular velocity and angular momentum than the merging point between the fat and thin plasma rings, a feature we verified to be valid independently of the choice for the energy of the system.

Alternatively, we could represent the new phase in the $\tilde{S}-\tilde{J}$ phase diagram. We get $(d\tilde{S}/d\tilde{J})^{(2)} = 0$ up to second order terms (this is not a surprise since at the order we work, the entropy is equal to the energy). Now, in the classical regime, the plasma family also has zero slope for this quantity so in principle one should go to higher order in ϵ if we wish to compute accurately the slope of the m -lobed family. In our approximation the bifurcation point tends to collapse to the static plasma ball point in the $\tilde{S}-\tilde{J}$ diagram where the slope vanishes. Therefore, at the order we work, the representation in this diagram is not a good choice.

The current line of research is not exhausted in the present analysis. In future work, it should be certainly possible to find numerically the full branch of non-axisymmetric plasma lumps in the phase diagram, and to discuss their stability.

6 Unstable plasma balls and their dual black holes

In the previous two sections we found that, starting with a static plasma ball, as we increase its rotation, the axisymmetric rotating plasma ball becomes unstable first to a 2-lobed perturbation and then to $m > 2$ lobed perturbations. Moreover, the marginal unstable modes were found to be bifurcation points in the phase diagram of solutions to a new branch of m -lobed plasma lumps. It is important to emphasize that these new plasma phases inhabit a region in parameter space where hydrodynamics provides a reliable holographic description of the dual gravitational system. This dual system was discussed in the Introduction: in the long wavelength regime, $3d$ fluid dynamics is an effective theory describing the Scherk-Schwarz (SS) compactification of a $4d$ CFT. The latter is dual to the SS compactification of AdS_5 gravity. It then follows that $3d$ plasma lumps correspond, in the dual gravity description, to SS AdS_5 black objects. The axisymmetric plasma balls and plasma rings correspond, respectively, to rotating black holes and black rings in SS AdS_5 [21].

Since plasma balls are unstable above a critical rotation rate (cf. Section 4), the holographic dual SS AdS_5 black holes must also be unstable against m -lobed perturbations. These axisymmetric black holes are expected to bifurcate to a new branch of *non-axisymmetric* black hole solutions in accordance with the plasma results. In the simplest $m = 2$ case, these are non-axisymmetric solutions that describe a peanut-like rigidly rotating black hole. Such a deformed black hole must necessarily emit all kinds of radiation. These waves can escape to infinity through the directions parallel to the holographic boundary (where the dual fluid lives). It is then natural to expect that this non-axisymmetric black hole will decay, probably emitting a good amount of the angular momentum and multipoles of the system, into an axisymmetric slowly rotating black hole.⁸ In practice, this instability provides then a mechanism that constraints the rotation of the black hole: effectively it introduces an upper bound for the rotation of the SS black hole. Some of these non-axisymmetric black holes are expected to decay very slowly and to be long-lived. Indeed it is important to emphasize that hydrodynamics can only provide a good description of a gravitational system in a regime where the gravitational interaction and radiation is suppressed. For example, two plasma balls do not interact and their collision is not accompanied by radiation emission, so they can only describe approximately two black holes when they are widely separated. Therefore, in the regime where our fluid description provides a good approximation, we should expect radiation emission to be suppressed in the dual gravitational system. Thus the non-axisymmetric black holes should indeed be long-lived, leaking very slowly radiation and angular momentum. Finding the explicit geometry describing such a solution will probably require a full-blown numerical solution of the field equations. This is thus a valuable example of the power of the hydrodynamic/gravity duality.

We expect our main conclusions to extend to higher dimensional theories as well. For any $d \geq 3$, d -dimensional fluid dynamics is an effective theory describing the SS compactification of a $(d + 1)$ -dimensional CFT, which is dual to a SS compactification of AdS_{d+2} . Apart from an expected simplification of the technical analysis in the $d = 3$ case, there is clearly no step in our analysis that is valid only for $d = 3$. Thus, plasma balls and dual black holes rotating above a

⁸We are undoubtedly grateful to Roberto Emparan for fruitful discussions concerning the dual interpretation of the plasma results

critical rate should also be unstable in higher dimensions and bifurcate to m -lobed plasmas and black holes. But, as we discuss in the sequel, we also expect some significant differences between the $d = 3$ and $d > 3$ cases.

Eventually new features are expected as one climbs the dimensionality ladder. For instance, new plasma lump configurations appear for $d > 3$. Indeed, in $d > 3$ one can have, besides the configurations discussed here, also pinched plasma balls, non-uniform tubes and pinched non-uniform tubes [21, 22, 28]. In the dual gravitational system, pinched balls [22] correspond to pinched black holes [35], and the non-uniform tubes describe non-uniform black strings with the pinched ones being black strings on the verge of expelling a black ring [28]. It would be quite interesting to understand the stability properties and phase diagrams of plasma balls in higher dimensions.

But, the results of the present analysis already allow one to infer important properties about the stability and existence of new solutions in higher dimensions. Consider hydrodynamics in a $d = 4$ Minkowski background (the boundary of SS AdS₆ black objects). Take a static plasma tube with topology $D^2 \times \mathbb{R}$ or $D^2 \times S^1$ (it is translationally invariant along the extra direction which can be or not compact). Such a plasma tube is unstable against the Rayleigh-Plateau instability when its length is larger than its transverse perimeter [4, 5, 28]. In the dual system, the corresponding black string is Gregory-Laflamme unstable [3], the holographic dual of the fluid instability. The marginal unstable mode is a bifurcation point to a new phase of solutions describing non-uniform plasma tubes and black strings. For details of this instability, see Refs. [4, 5, 13, 28, 36]. Now, a $4d$ static plasma tube is simply a $3d$ plasma ball trivially extended along the extra direction. Our results then show that a rotating plasma tube, with the rotation axis along the tube direction, should also be unstable, above a critical rotation rate, to m -lobed perturbations. Moreover, the marginally stable points are bifurcation points, this time to non-axisymmetric plasma tubes translationally invariant along the tube direction and whose transverse cross section has a m -lobed shape. Again, by the hydrodynamic/gravity duality, we expect that rotating black strings will become unstable, not only against the Gregory-Laflamme instability, but also against m -lobed azimuthal perturbations. And a new branch of non-axisymmetric m -lobed black strings is expected to branch-off at the unstable threshold point in the phase diagram of solutions. Other interesting solutions include axisymmetric non-uniform black strings (these bifurcate from the Gregory-Laflamme unstable point) and pinched non-uniform black strings which are also solutions of the gravity theory [28]. Our study then predicts the existence of non-axisymmetric non-uniform black strings and pinched ones. We emphasize that the existence of pinched black strings [28] and non-axisymmetric m -lobed black strings would hardly be anticipated without resorting to the hydrodynamic/gravity duality. Our discussion focused on $4d$ plasma tubes dual to $6d$ black strings but again it should extend to higher dimensions.

These results rely on the hydrodynamic description of a particular gauge/gravity duality, namely of the Scherk-Schwarz system. Experience with hydrodynamics indicates that similar results should be found for other gauge/gravity theories with an effective hydrodynamic description and a confinement/deconfinement phase transition. The deconfined black hole phase of such a general system is still expected to be described at leading order by a perfect fluid holographic stress tensor, and the interface between the deconfined and confined phases is again expected to be dictated by a domain wall with a surface tension. Such a generic dual system will of course have a different equation

of state, encoding the information on the kind of fluid describing the gauge theory. However, our analysis is not very sensitive to the particular equation of state of the plasma. Hence it could be that our main results on the stability and bifurcation properties of plasma balls will be common to generic dualities.

It would also be interesting to investigate the dual of the superradiant instability on the plasma balls. In general, rotating black holes develop an ergoregion, a region in spacetime with negative energy states. For spacetimes with ergoregions, one can have superradiant scattering, whereby a wave (with frequency $\omega < m\Omega$, where m is an azimuthal number and Ω is the horizon velocity) can be amplified, extracting rotational energy from the hole. In AdS, the superradiantly amplified waves bounce back at infinity and lead to a superradiant instability [43]. Thus four- [42, 44] and higher dimensional [45, 46] rotating Kerr-AdS black holes can be unstable. The endpoint of such an instability is presumably an element of a new branch of stationary black holes, rotating in such a way as to avoid the superradiant window [45, 42]. Some of the angular momentum of the black hole is transferred to caged radiation in between the horizon and the AdS wall and co-rotating with the black hole. It was also argued in [45] that a new branch of non-axisymmetric black hole solutions could eventually bifurcate from the original Kerr-AdS black hole at the threshold of the superradiant instability. This superradiant phenomena is a similar, but not identical, mechanism to the one we explored in this paper (the mechanism dealt with here is not dependent on superradiant amplification). They may correspond to different bifurcation branches in a phase diagram of possible solutions. To explore the eventual dual of the superradiant instability on a plasma ball we should take into account that experience indicates that an ergoregion instability develops when the rotation speed at the boundary surface, ΩR_o , exceeds the sound speed of the plasma. This then corresponds to the formation of an acoustic “ergoregion” in the system, and therefore by a general theorem by Friedman [47], they should be unstable. We should however keep in mind a possible serious caveat: the dual hydrodynamic description is typically valid for large AdS black holes (*i.e.*, for those whose horizon is large compared with the cosmological scale) [21, 30], while the superradiant instability is present only in small AdS black holes [42, 44]. So it might well be that the fluid description is not able to capture the dual of the superradiant instability.

7 Acknowledgments

We warmly thank Marco Caldarelli, Roberto Emparan and Dietmar Klemm for very fruitful discussions, and Roberto Emparan for his useful comments to the final version of this manuscript. We also thank CERN for hospitality during the programme “Black Holes: A Landscape of Theoretical Physics Problems”, August-October 2008, where part of this work was done. OJCD further acknowledges the University of Barcelona where this work started and the organizers of the workshop “Higher dimensional black holes: Exact solutions and their stability”, Laboratoire de Physique Théorique, France. This work was partially funded by Fundação para a Ciência e Tecnologia (FCT) - Portugal through projects PTDC/FIS/64175/2006 and CERN/FP/83508/2008. VC acknowledges financial support through a Fulbright Scholarship. OJCD acknowledges financial support provided by the European Community through the Intra-European Marie Curie contract MEIF-CT-2008.

Appendices

A On the stability of plasma rings

In this Appendix we discuss the stability of plasma rings, and we find that plasma rings are *stable* against the *particular* m -lobed deformations that we consider. Plasma rings have an inner boundary at $r = R_i$ in addition to the outer boundary at $r = R_o$. The boundary conditions (4.12) and (4.10) yield the following system for the outer and inner surfaces,

$$U_r(R_{o,i}) = \frac{\omega R_{o,i}^2 \gamma_{o,i}^8}{\sigma \left[\pm \left(\frac{1}{c^2} (\omega - im\Omega)^2 R_{o,i}^2 + m^2 - 1 \right) - \frac{4\rho_*}{3} \frac{\Omega^2 R_{o,i}^3}{\sigma} \gamma_{o,i}^6 \right]} \mathcal{P}(R_{o,i}). \quad (\text{A.1})$$

Relations (4.7) and (A.1) provide two conditions on \mathcal{P} and constitute again an eigenvalue problem for ω . The problem depends on two dimensionless quantities: $\frac{\rho_* R_o}{\sigma}$ and ΩR_o . For $\Omega R_o \ll c$, (4.8) and (4.7) reduce respectively to (4.15) and (4.16), while (A.1) simplifies to

$$U_r(R_{o,i}) = \frac{\omega R_{o,i}^2}{\sigma \left(\pm (m^2 - 1) - \frac{4\rho_*}{3} \frac{\Omega^2 R_{o,i}^3}{\sigma} \right)} \mathcal{P}(R_{o,i}). \quad (\text{A.2})$$

For black rings some of these quantities are not independent, *e.g.*, we have $R_i = R_i(R_o)$ and $\Omega = \Omega(R_o, \rho/\sigma)$. In section 3 we already discussed these constraints so it is appropriate to rewrite (4.15), (4.16) and (A.2) in terms of the dimensionless variables (3.2). Defining also the dimensionless frequency $\tilde{\omega} = \frac{\sigma}{\rho_0} \omega$ the system we have to solve is

$$\mathcal{P}(v) = Av^m + Bv^{-m}, \quad (\text{A.3})$$

$$-\tilde{\Omega}^2 \frac{2im\tilde{\Omega}\mathcal{P}(v_o) + \tilde{\omega}v_o\mathcal{P}'(v_o)}{4vg_+(v_o) \left(\tilde{\omega}^2 + 4\tilde{\Omega}^2 \right)} = \frac{\tilde{\omega}}{\tilde{\Omega}} \frac{v_o^2}{\left[\pm (m^2 - 1) - \frac{4}{\tilde{\Omega}} g_+(v_o)v_o^3 \right]} \mathcal{P}(v_o), \quad (\text{A.4})$$

$$-\tilde{\Omega}^2 \frac{2im\tilde{\Omega}\mathcal{P}(v_i) + \tilde{\omega}v_i\mathcal{P}'(v_i)}{4vg_-(v_i) \left(\tilde{\omega}^2 + 4\tilde{\Omega}^2 \right)} = \frac{\tilde{\omega}}{\tilde{\Omega}} \frac{v_i^2}{\left[\pm (m^2 - 1) - \frac{4}{\tilde{\Omega}} g_-(v_i)v_i^3 \right]} \mathcal{P}(v_i). \quad (\text{A.5})$$

We have found no unstable mode. One might argue that black rings should be unstable at least at the point where they cross that plasma ball diagram of Fig. 7. This does not necessarily have to be in contradiction with our results first because the boundary conditions for black rings do not seem to reduce to the boundary conditions for plasma balls, even in this limit. Second, the analysis here does not prove that these plasma rings are stable: they are stable against the particular m -lobed deformations that we consider (see discussion just after (4.9)). A more general analysis is needed, encompassing generic perturbations.

References

- [1] J. Plateau, *Statique Expérimentale et Théorique des Liquides Soumis aux Seules Forces Moléculaires*, (Paris, Gauthier-Villars, 1873).

- [2] N. Bohr and J. A. Wheeler, “The mechanism of nuclear fission,” *Phys. Rev.* **56**, 426 (1939);
C. Y. Wong, “Toroidal and spherical bubble nuclei,” *Annals of Physics (NY)* **77**, 279 (1973).
- [3] R. Gregory and R. Laflamme, “Black strings and p-branes are unstable,” *Phys. Rev. Lett.* **70**, 2837 (1993) [arXiv:hep-th/9301052].
- [4] V. Cardoso and O. J. C. Dias, “Gregory-Laflamme and Rayleigh-Plateau instabilities,” *Phys. Rev. Lett.* **96**, 181601 (2006) [arXiv:hep-th/0602017].
- [5] V. Cardoso and L. Gualtieri, “Equilibrium configurations of fluids and their stability in higher dimensions,” *Class. Quant. Grav.* **23** (2006) 7151 [arXiv:hep-th/0610004];
V. Cardoso, O. J. C. Dias and L. Gualtieri, “The return of the membrane paradigm? Black holes and strings in the water tap,” *Int. J. Mod. Phys. D* **17**, 505 (2008) [arXiv:0705.2777 [hep-th]].
- [6] E. Fermi, “High-energy nuclear events,” *Prog. Theor. Phys.* **5**, 570 (1950).
- [7] L. D. Landau, “On the multiparticle production in high-energy collisions,” *Izv. Akad. Nauk Ser. Fiz.* **17**, 51 (1953).
- [8] L.D. Landau and E.M. Lifshitz, *Fluid Mechanics* (Pergamon Press, New York, 1987), 2nd ed.
- [9] G. Policastro, D. T. Son and A. O. Starinets, “The shear viscosity of strongly coupled $N = 4$ supersymmetric Yang-Mills plasma,” *Phys. Rev. Lett.* **87**, 081601 (2001) [arXiv:hep-th/0104066];
G. Policastro, D. T. Son and A. O. Starinets, “From AdS/CFT correspondence to hydrodynamics,” *JHEP* **0209**, 043 (2002) [arXiv:hep-th/0205052];
D. T. Son and A. O. Starinets, “Viscosity, Black Holes, and Quantum Field Theory,” *Ann. Rev. Nucl. Part. Sci.* **57** (2007) 95 [arXiv:0704.0240 [hep-th]].
- [10] S. Bhattacharyya, V. E. Hubeny, S. Minwalla and M. Rangamani, “Nonlinear Fluid Dynamics from Gravity,” *JHEP* **0802** (2008) 045 [arXiv:0712.2456 [hep-th]].
- [11] S. Bhattacharyya *et al.*, “Local Fluid Dynamical Entropy from Gravity,” *JHEP* **0806** (2008) 055 [arXiv:0803.2526 [hep-th]].
- [12] M. Van Raamsdonk, “Black Hole Dynamics From Atmospheric Science,” *JHEP* **0805** (2008) 106 [arXiv:0802.3224 [hep-th]];
S. Bhattacharyya, R. Loganayagam, S. Minwalla, S. Nampuri, S. P. Trivedi and S. R. Wadia, “Forced Fluid Dynamics from Gravity,” arXiv:0806.0006 [hep-th];
M. Haack and A. Yarom, “Nonlinear viscous hydrodynamics in various dimensions using AdS/CFT,” *JHEP* **0810** (2008) 063 [arXiv:0806.4602 [hep-th]];
S. Bhattacharyya, R. Loganayagam, I. Mandal, S. Minwalla and A. Sharma, “Conformal Non-linear Fluid Dynamics from Gravity in Arbitrary Dimensions,” arXiv:0809.4272 [hep-th];
J. Erdmenger, M. Haack, M. Kaminski and A. Yarom, “Fluid dynamics of R-charged black holes,” arXiv:0809.2488 [hep-th];
N. Banerjee, J. Bhattacharya, S. Bhattacharyya, S. Dutta, R. Loganayagam and P. Surowka,

- “Hydrodynamics from charged black branes,” arXiv:0809.2596 [hep-th];
M. Haack and A. Yarom, “Universality of second order transport coefficients from the gauge-string duality,” arXiv:0811.1794 [hep-th];
J. Hansen and P. Kraus, “Nonlinear Magnetohydrodynamics from Gravity,” arXiv:0811.3468 [hep-th].
- [13] M. M. Caldarelli, O. J. C. Dias and D. Klemm, “Dyonic AdS black holes from magnetohydrodynamics,” arXiv:0812.0801 [hep-th].
- [14] I. R. Klebanov and J. M. Maldacena, “Solving quantum field theories via curved spacetimes,” *Physics Today*, pp. 28-33 (January, 2009);
C. Csaki, M. Reece and J. Terning, “The AdS/QCD Correspondence: Still Undelivered,” arXiv:0811.3001 [hep-ph];
R. C. Myers and S. E. Vazquez, “Quark Soup al dente: Applied Superstring Theory,” *Class. Quant. Grav.* **25** (2008) 114008 [arXiv:0804.2423 [hep-th]].
- [15] S. S. Gubser and A. Karch, “From gauge-string duality to strong interactions: a Pedestrian’s Guide,” arXiv:0901.0935 [hep-th].
- [16] E. Witten, “Anti-de Sitter space, thermal phase transition, and confinement in gauge theories,” *Adv. Theor. Math. Phys.* **2** (1998) 505 [arXiv:hep-th/9803131];
D. Mateos, “String Theory and Quantum Chromodynamics,” *Class. Quant. Grav.* **24** (2007) S713 [arXiv:0709.1523 [hep-th]].
- [17] M. Kruczenski, D. Mateos, R. C. Myers and D. J. Winters, “Towards a holographic dual of large- $N(c)$ QCD,” *JHEP* **0405** (2004) 041 [arXiv:hep-th/0311270].
- [18] T. Sakai and S. Sugimoto, “Low energy hadron physics in holographic QCD,” *Prog. Theor. Phys.* **113** (2005) 843 [arXiv:hep-th/0412141].
- [19] G. T. Horowitz and R. C. Myers, “The AdS/CFT Correspondence and a New Positive Energy Conjecture for General Relativity,” *Phys. Rev. D* **59** (1998) 026005 [arXiv:hep-th/9808079].
- [20] O. Aharony, S. Minwalla and T. Wiseman, “Plasma-balls in large N gauge theories and localized black holes,” *Class. Quant. Grav.* **23** (2006) 2171 [arXiv:hep-th/0507219].
- [21] S. Lahiri and S. Minwalla, “Plasmarings as dual black rings,” arXiv:0705.3404 [hep-th].
- [22] S. Bhardwaj and J. Bhattacharya, “Thermodynamics of Plasmaballs and Plasmarings in 3+1 Dimensions,” arXiv:0806.1897 [hep-th].
- [23] S. Chandrasekhar, “The stability of a rotating liquid drop,” *Proc. Roy. Soc. Ser. A* **286**, 1 (1965).
- [24] R. A. Brown and L. E. Scriven, “The shape and stability of rotating liquid drops,” *Proc. Roy. Soc. London Ser. A* **371**, 331 (1980).

- [25] V. Cardoso, “The many shapes of spinning drops”, *Physics* **1**, 38 (2008).
- [26] R. J. A. Hill and L. Eaves, “Polygonal excitations of spinning and levitating droplets”, arXiv:0808.3704 [physics].
- [27] A. V Lebedev, A. Engel, K. I Morozov and H. Bauke, “Ferrofluid drops in rotating magnetic fields”, *New J. Phys.* **5**, 57 (2003).
- [28] M. M. Caldarelli, O. J. C. Dias, R. Emparan and D. Klemm, “Black holes as lumps of fluid,” arXiv:0811.2381 [hep-th].
- [29] S. Chandrasekhar, “Solutions of two problems in the theory of gravitational radiation,” *Phys. Rev. Lett.* **24**, 611 (1970).
- [30] S. Bhattacharyya, S. Lahiri, R. Loganayagam and S. Minwalla, “Large rotating AdS black holes from fluid mechanics,” arXiv:0708.1770 [hep-th].
- [31] L. M. Hocking, “The stability of a rigidly rotating column of liquid,” *Mathematika* **7**, 1 (1960);
L. M. Hocking and D. H. Michael, “The stability of a column of rotating liquid,” *Mathematika* **6**, 25 (1959);
J. Gillis, “Stability of a column of rotating viscous liquid,” *Proc. Camb. Phil. Soc.* **57**, 152 (1961);
J. P. Kubitschek and P. D. Weidman, The effect of viscosity on the stability of a uniformly rotating liquid column in zero gravity, *J. Fluid Mech.* **572**, 261 (2007).
- [32] P. Kovtun, D. T. Son and A. O. Starinets, “Viscosity in strongly interacting quantum field theories from black hole physics,” *Phys. Rev. Lett.* **94**, 111601 (2005);
P. Kovtun, D. T. Son and A. O. Starinets, “Holography and hydrodynamics: diffusion on stretched horizons,” *JHEP* **0310**, 064 (2003).
- [33] R. E. Benner, O. A. Basaran, L. E. Scriven, “Equilibria, Stability and Bifurcations of Rotating Columns of Fluid Subjected to Planar Disturbances,” *Proc. Math. and Phys. Sciences* **433** (1991) 81. Available at: <http://www.jstor.org/stable/51936>
- [34] I. Fouxon and Y. Oz, “Conformal Field Theory as Microscopic Dynamics of Incompressible Euler and Navier-Stokes Equations,” arXiv:0809.4512 [hep-th];
S. Bhattacharyya, S. Minwalla and S. R. Wadia, “The Incompressible Non-Relativistic Navier-Stokes Equation from Gravity,” arXiv:0810.1545 [hep-th].
- [35] R. Emparan and R. C. Myers, “Instability of ultra-spinning black holes,” *JHEP* **0309** (2003) 025 [arXiv:hep-th/0308056].
- [36] K. i. Maeda and U. Miyamoto, “Black hole-black string phase transitions from hydrodynamics,” arXiv:0811.2305 [hep-th].
- [37] M. M. Caldarelli, R. Emparan and M. J. Rodriguez, “Black Rings in (Anti)-deSitter space,” *JHEP* **0811** (2008) 011 [arXiv:0806.1954 [hep-th]].

- [38] S. Hollands, A. Ishibashi and R. M. Wald, “A higher dimensional stationary rotating black hole must be axisymmetric,” *Commun. Math. Phys.* **271**, 699 (2007) [arXiv:gr-qc/0605106].
- [39] R. C. Myers and M. J. Perry, “Black Holes In Higher Dimensional Space-Times,” *Annals Phys.* **172** (1986) 304.
- [40] R. Emparan and H. S. Reall, “A rotating black ring in five dimensions,” *Phys. Rev. Lett.* **88** (2002) 101101 [arXiv:hep-th/0110260].
- [41] H. K. Kunduri and J. Lucietti, “Uniqueness of near-horizon geometries of rotating extremal AdS(4) black holes,” arXiv:0812.1576 [hep-th].
- [42] V. Cardoso, O. J. C. Dias and S. Yoshida, “Classical instability of Kerr-AdS black holes and the issue of final state,” *Phys. Rev. D* **74** (2006) 044008 [arXiv:hep-th/0607162].
- [43] V. Cardoso, O. J. C. Dias, J. P. S. Lemos and S. Yoshida, “The black hole bomb and super-radiant instabilities,” *Phys. Rev. D* **70**, 044039 (2004) [Erratum-ibid. *D* **70**, 049903 (2004)] [arXiv:hep-th/0404096].
- [44] V. Cardoso and O. J. C. Dias, “Small Kerr-anti-de Sitter black holes are unstable,” *Phys. Rev. D* **70** (2004) 084011 [arXiv:hep-th/0405006];
- [45] H. K. Kunduri, J. Lucietti and H. S. Reall, “Gravitational perturbations of higher dimensional rotating black holes: Tensor Perturbations,” *Phys. Rev. D* **74** (2006) 084021 [arXiv:hep-th/0606076];
- [46] H. Kodama, “Superradiance and Instability of Black Holes,” *Prog. Theor. Phys. Suppl.* **172**, 11 (2008) [arXiv:0711.4184 [hep-th]];
A. N. Aliev and O. Delice, “Superradiant Instability of Five-Dimensional Rotating Charged AdS Black Holes,” arXiv:0808.0280 [hep-th];
H. Kodama, R. A. Konoplya and A. Zhidenko, “Gravitational instability of simply rotating Myers-Perry-AdS black holes,” arXiv:0812.0445 [hep-th];
K. Murata, “Instabilities of Kerr-AdS₅ × S⁵ Spacetime,” arXiv:0812.0718 [hep-th].
- [47] J. L. Friedman, “Ergosphere instability”, *Commun. Math. Phys.* **63**, 243 (1978);
V. Cardoso, O. J. C. Dias, J. L. Hovdebo and R. C. Myers, “Instability of non-supersymmetric smooth geometries,” *Phys. Rev. D* **73**, 064031 (2006) [arXiv:hep-th/0512277].